JGR Atmospheres

RESEARCH ARTICLE
10.1029/2023JD039257

Implications of Snowpack Reactive Bromine Production for Arctic Ice Core Bromine Preservation

Shuting Zhai[1], William Swanson[2], Joseph R. McConnell[3], Nathan Chellman[3], Thomas Opel[4], Michael Sigl[5], Hanno Meyer[4], Xuan Wang[6,7], Lyatt Jaeglé[1], Jochen Stutz[8,9], Jack E. Dibb[10], Koji Fujita[11], and Becky Alexander[1]

[1]Department of Atmospheric Sciences, University of Washington, Seattle, WA, USA, [2]Department of Chemistry and Biochemistry and Geophysical Institute, University of Alaska Fairbanks, Fairbanks, AK, USA, [3]Division of Hydrologic Sciences, Desert Research Institute, Reno, NV, USA, [4]Alfred Wegener Institute Helmholtz Centre for Polar and Marine Research, Potsdam, Germany, [5]Climate and Environmental Physics, University of Bern, Bern, Switzerland, [6]School of Energy and Environment, City University of Hong Kong, Hong Kong SAR, China, [7]City University of Hong Kong Shenzhen Research Institute, Shenzhen, China, [8]University of California, Los Angeles, CA, USA, [9]Department of Atmospheric and Oceanic Sciences, Los Angeles, CA, USA, [10]Institute for the Study of Earth, Oceans and Space, University of New Hampshire, Durham, NH, USA, [11]Graduate School of Environmental Studies, Nagoya University, Nagoya, Japan

Key Points:

- Ice-core and model analysis suggest that the Russian Arctic Akademii Nauk ice core preserves atmospheric bromine signals since preindustrial
- Bromine loss from snow is potentially significant in inland Greenland and should be considered when interpreting ice core bromine records

Supporting Information:

Supporting Information may be found in the online version of this article.

Correspondence to:

B. Alexander,
beckya@uw.edu

Citation:

Zhai, S., Swanson, W., McConnell, J. R., Chellman, N., Opel, T., Sigl, M., et al. (2023). Implications of snowpack reactive bromine production for Arctic ice core bromine preservation. *Journal of Geophysical Research: Atmospheres*, *128*, e2023JD039257. https://doi.org/10.1029/2023JD039257

Received 16 MAY 2023
Accepted 5 OCT 2023

Author Contributions:

Conceptualization: Shuting Zhai, Joseph R. McConnell, Becky Alexander
Data curation: Shuting Zhai, Joseph R. McConnell, Nathan Chellman, Thomas Opel, Michael Sigl, Jochen Stutz, Jack E. Dibb, Koji Fujita, Becky Alexander
Formal analysis: Shuting Zhai, Joseph R. McConnell, Nathan Chellman, Thomas Opel, Michael Sigl, Hanno Meyer, Koji Fujita, Becky Alexander
Funding acquisition: Shuting Zhai, Becky Alexander
Investigation: Shuting Zhai, Joseph R. McConnell, Nathan Chellman, Jochen Stutz, Jack E. Dibb, Becky Alexander
Methodology: Shuting Zhai, William Swanson, Joseph R. McConnell, Nathan Chellman, Thomas Opel, Michael Sigl, Hanno Meyer, Xuan Wang, Lyatt Jaeglé, Koji Fujita, Becky Alexander
Project Administration: Becky Alexander

Abstract Snowpack emissions are recognized as an important source of gas-phase reactive bromine in the Arctic and are necessary to explain ozone depletion events in spring caused by the catalytic destruction of ozone by halogen radicals. Quantifying bromine emissions from snowpack is essential for interpretation of ice-core bromine. We present ice-core bromine records since the pre-industrial (1750 CE) from six Arctic locations and examine potential post-depositional loss of snowpack bromine using a global chemical transport model. Trend analysis of the ice-core records shows that only the high-latitude coastal Akademii Nauk (AN) ice core from the Russian Arctic preserves significant trends since pre-industrial times that are consistent with trends in sea ice extent and anthropogenic emissions from source regions. Model simulations suggest that recycling of reactive bromine on the snow skin layer (top 1 mm) results in 9–17% loss of deposited bromine across all six ice-core locations. Reactive bromine production from below the snow skin layer and within the snow photic zone is potentially more important, but the magnitude of this source is uncertain. Model simulations suggest that the AN core is most likely to preserve an atmospheric signal compared to five Greenland ice cores due to its high latitude location combined with a relatively high snow accumulation rate. Understanding the sources and amount of photochemically reactive snow bromide in the snow photic zone throughout the sunlit period in the high Arctic is essential for interpreting ice-core bromine, and warrants further lab studies and field observations at inland locations.

Plain Language Summary Bromine is a reactive chemical species emitted from natural and anthropogenic sources and can be reemitted from Arctic snowpack after its deposition on snow. This leads to ozone depletion and alters the record of bromine preserved in ice cores. Here, we studied ice-core records of bromine from six Arctic locations to quantify the extent of bromine loss from the snowpack since the pre-industrial era. We found that only one location had significant trends of bromine over time, consistent with trends in bromine sources from both nature and human activities. An atmospheric model including chemical reaction processes suggested that this Russian Arctic location favored preservation of bromine compared to the five Greenland ice cores. Understanding bromine preservation in Arctic snow and ice is important for interpreting ice-core records.

1. Introduction

Tropospheric reactive bromine (Br_y = Br + $2Br_2$ + HOBr + BrO + HBr + $BrNO_2$ + $BrNO_3$ + IBr + BrCl) impacts the oxidizing capacity of the atmosphere by depleting ozone and perturbing OH to HO_2 ratios toward OH (von Glasow et al., 2004; Sherwen et al., 2016). In polar regions, Br_y is largely responsible for surface ozone depletion events (ODEs) in coastal regions in the spring (Barrie et al., 1988; Oltmans et al., 1989, 2012). Reactive iodine also plays a role in ODEs (Benavent et al., 2022), with a smaller contribution from reactive chlorine (Wang et al., 2021). Br_y is also associated with atmospheric mercury depletion events in the Arctic (Horowitz et al., 2017; Steffen et al., 2008).

Resources: Shuting Zhai, Joseph R. McConnell, Jochen Stutz, Becky Alexander
Software: Shuting Zhai, William Swanson, Xuan Wang, Lyatt Jaeglé, Koji Fujita, Becky Alexander
Supervision: Becky Alexander
Validation: Shuting Zhai, Michael Sigl, Lyatt Jaeglé, Jochen Stutz, Jack E. Dibb, Becky Alexander
Visualization: Shuting Zhai, Becky Alexander
Writing – original draft: Shuting Zhai, Becky Alexander
Writing – review & editing: Shuting Zhai, William Swanson, Joseph R. McConnell, Nathan Chellman, Thomas Opel, Michael Sigl, Hanno Meyer, Xuan Wang, Lyatt Jaeglé, Jochen Stutz, Jack E. Dibb, Koji Fujita, Becky Alexander

Major sources of tropospheric reactive bromine include sea salt aerosol (SSA) debromination (Kerkweg et al., 2008; Yang et al., 2005), emissions of organobromine species from the marine biosphere (Liang et al., 2010; Quack & Wallace, 2003), emissions from saline lakes (Hebestreit et al., 1999; Matveev et al., 2001), and volcanoes (Aiuppa et al., 2005; Bobrowski et al., 2003). Anthropogenic-related sources of Br_y include agricultural emissions (Clerbaux et al., 2007), emissions from vehicles using leaded gasoline (Habibi, 1973; Thomas et al., 1997), coal combustion (Lee et al., 2018), biomass burning (Reeves, 2003), and stratospheric transport from degradation of organobromines and halons (Liang et al., 2014). In the Arctic, debromination of SSA originating from blowing snow (Huang et al., 2020; Yang et al., 2008) and direct emissions of reactive bromine from snowpack have been observed (Abbatt et al., 2012; Dibb et al., 2010; Foster et al., 2001; Pratt et al., 2013; Simpsonet al., 2007a, 2007b; Stutz et al., 2011) and are necessary to explain depletion of surface ozone in the spring (Lehrer et al., 2004; Michalowski et al., 2000; Piot & von Glasow, 2008; Swanson et al., 2022).

The major sink of tropospheric Br_y is uptake by aerosols, and both Br_y and aerosol bromide are removed from the atmosphere through wet and dry deposition to the surface. Bromine in snowpack originates from deposition of gaseous and aerosol phase bromine. Bromine in snow over first year sea ice has additional sources from wind-blown frost flowers and upward migration from sea ice (Domine et al., 2004). Deposition of bromine to the cryosphere is reversible due to snowpack bromine chemistry, potentially affecting the preservation of bromine in ice cores (McConnell et al., 2017; Vallelonga et al., 2021). Ice-core bromine records have been interpreted to reflect changes in sea ice extent (Maffezzoli et al., 2021; Spolaor et al., 2013a, 2013b, 2016a, 2016b), atmospheric acidity (Maselli et al., 2017), and anthropogenic bromine emissions (Legrand et al., 2021) under the assumption that bromine species are well preserved in ice cores with high snow accumulation rates typical of the Arctic and mid-latitudes. Understanding the magnitude and mechanisms of snowpack reactive bromine release is important for interpretation of ice-core bromine measurements.

Snowpack emissions of reactive bromine involve both gas-phase and heterogeneous chemistry across the atmosphere-snowpack interface. Gas-phase reactions that occur in the atmosphere (R 1–5) also occur in the snowpack interstitial air (SIA) (Pratt et al., 2013; Toyota et al., 2014).

$$O_3 + Br \rightarrow BrO + O_2 \quad (R1)$$

$$HO_2 + BrO \rightarrow HOBr + O_2 \quad (R2)$$

$$HOBr + h\upsilon \rightarrow OH + Br \quad (R3)$$

$$\text{Net}: HO_2 + O_3 \rightarrow 2O_2 + OH$$

$$BrO + NO_2 + M \rightarrow BrNO_3 + M \quad (R4)$$

$$BrNO_3 + HO_2O(liq) \rightarrow HOBr + HNO_3(aq) \quad (R5)$$

$$2OH(aq) + 2Br^-(aq) + 2H^+(aq) \rightarrow Br_2 + 2H_2O(aq) \quad (R6)$$

$$O_3(aq) + Br^-(aq) + H^+(aq) \rightarrow HOBr(aq) + O_2(aq) \quad (R7)$$

$$BrNO_3 + HO_2O(liq) \rightarrow HOBr(aq) + H^+(aq) + NO_3^-(aq) \quad (R8)$$

$$HOBr(aq) + X^-(aq) + H^+(aq) \rightarrow BrX + HO_2O(aq) \quad (R9)$$

Similar to bromide (Br^-) in SSA, Br^- at the surface of snow grains can be oxidized by OH (R6) and O_3 (R7) or react with $BrNO_3$ (R8, R9) and HOBr (R9) to form BrX (where X = Br or Cl) (R6–9). Since bromide is expected to be enhanced at the snow grain surface (Ghosal et al., 2000, 2005; Gladich et al., 2011) relative to bulk snow, and Br^- reacts much faster with OH compared to Cl^- (Abbatt et al., 2010), Br_2 and BrCl are preferentially formed compared to Cl_2 (Custard et al., 2017). Preferential production of Br_2 over BrCl was shown in lab studies for snow with high Br^-/Cl^- ratios (Sjostedt & Abbatt, 2008). The resulting BrX can transfer to SIA and mix with the atmosphere above via wind pumping and gas-phase diffusion (Thomas et al., 2011; Toyota et al., 2014). These reaction pathways are largely photochemically driven. Possible dark reaction mechanisms include heterogeneous reactions of Br^- with HOBr, $BrNO_3$, and O_3 (R7–9). Another potentially important factor in heterogeneous reactions is snow acidity, since both bromine cycling within snowpack via R6, R7, and R9 and OH formation in the snowpack via nitrate photolysis are acid-catalyzed (McConnell et al., 2017; Mozurkewich, 1995).

Concentrations of Br_2 and BrCl in coastal Arctic surface air during spring have been observed to be as high as several tens of ppt (Foster et al., 2001; J. Liao et al., 2012, 2014; Spicer et al., 2002) and are thought to originate at least partially from snow emissions. Foster et al. (2001) first reported the release of photolabile bromine compounds from the snowpack at Alert, Canada by showing that measured molecular bromine (Br_2) in SIA just below the surface of the snowpack reached 2ppt, about twice that measured in the air above. Pratt et al. (2013) conducted an outdoor snow chamber experiment in Utqiagvik, Alaska and demonstrated that snow bromine release is facilitated by ozone-mediated photochemical production of Br_2 in snow with enhanced Br^-/Cl^- ratios and high acidity. Also at Utqiagvik, Custard et al. (2017) measured molecular halogens in SIA and calculated a mean emission flux of $\sim 5 \times 10^8$ molecules cm^{-2} s^{-1} and $\sim 3 \times 10^8$ molecules cm^{-2} s^{-1} for Br_2 and Cl_2, respectively, out of snowpack into the atmosphere. The study also reported up to 500 ppt of Br_2, up to 45 ppt of BrCl, and up to 25 ppt of Cl_2 in SIA at a snow depth of 10 cm under artificial irradiation conditions.

Elevated atmospheric BrO concentrations were also observed in inland Arctic. Peterson et al. (2018) observed enhanced BrO vertical column densities (VCD) 200 km from the coast of Utqiagvik, Alaska, especially near the surface of the snowpack. Stutz et al. (2011) reported elevated BrO (1–3 ppt) at Summit, Greenland in May, June, and July, even when the air mass was not from oceanic regions. During the same field campaign at Summit, Dibb et al. (2010) found that gas phase soluble Br^- measured in the pore spaces of firn air is higher than in the air above the snowpack, and that ambient Br^- peaks around local noon. These studies indicate that photochemical production of reactive bromine from local snowpack is the primary source of the observed BrO at inland locations.

To investigate the role of snow halogen chemistry in ODEs, several box models and 1D models were developed to simulate the dynamic interaction between snowpack and the overlying atmosphere. Although these models suffer uncertainties due to limited knowledge of snow microphysics and chemistry (Domine et al., 2013), they are useful for testing our understanding of the main sources of reactive bromine and causes of ODEs at specific locations and times. Using coupled 1D atmosphere-snow models at Summit, Greenland, Thomas et al. (2011, 2012a) and Toyota et al. (2014) found that bromine production from below the snow surface skin layer (top 1 mm, Erbland et al., 2013) dominates total snowpack emissions and is driven by photochemistry, which is highly dependent on the solar zenith angle (SZA) (Bourgeois et al., 2006; Grannas et al., 2007; Lee-Taylor & Madronich, 2002; Simpson et al., 2002; Warren, 1982). Snowpack emissions of bromine from the skin layer are driven by dry deposition of atmospheric HOBr, while deeper snowpack production (1–250 mm) is driven by both SIA Br_y chemistry (R1–5) and aqueous phase oxidation of bromide (R6–9) (Toyota et al., 2014). Piot and von Glasow (2009) used a box model to calculate the required fluxes of halogens to account for the observed effects on ozone in Alert, Canada in early spring, and estimated a Br_2 flux ranging from 5×10^7 to 1.5×10^9 molecules cm^{-2} s^{-1}. Other box and 1D modeling studies estimated maximum emissions of Br_2 of $2 - 5 \times 10^8$ molecules cm^{-2} s^{-1} at Utqiagvik, Alaska in March (Ahmed et al., 2022; Wang & Pratt, 2017), within the same order of magnitude of those from previous observation-based estimates from the same site (Custard et al., 2017).

Several global chemical transport models have incorporated snowpack bromine emissions to evaluate their role in explaining the spatiotemporal variability of ODEs across the Arctic. Toyota et al. (2011) implemented a snowpack chemistry mechanism in a 3D air quality model GEM-AQ by calculating the molar yield of BrX based on dry deposition of O_3, HOBr, and $BrNO_3$ for different snow types including first-year sea ice, multi-year sea ice, and land snow. The model was able to capture the spatial distribution of ODEs in April 2001 in the Arctic, and modestly agrees with satellite observations of BrO VCD. Although the GEM-AQ model does not explicitly include deeper snow production, the empirically determined molar yield parameters as a function of sunlight are meant to reflect influences from photochemically driven deeper production (Toyota et al., 2011). Falk and Sinnhuber (2018) applied the same framework in a global chemistry-climate model EMAC, and showed that the model was able to reproduce many bromine enhancements and ODEs in both hemispheres over a full annual cycle. Similar frameworks have been implemented recently in WRF-Chem (Herrmann et al., 2021, 2022; Marelle et al., 2021) and GEOS-Chem (Swanson et al., 2022), and good agreements were found between models and satellite and in situ observations of BrO and O_3 in coastal Arctic spring.

Most previous snowpack bromine studies were conducted for coastal Arctic sites during springtime, with a focus on springtime ODEs. For inland snow regions such as Greenland, previous global modeling studies predict negligible bromine production from the snowpack, either because of the assumption of minimal snow bromide replenishment from dry deposited HBr (Toyota et al., 2011), or a 500 m elevation filter to restrict inland snowpack emissions (Swanson et al., 2022). In this study, we examine inland Arctic sites, where most ice cores are

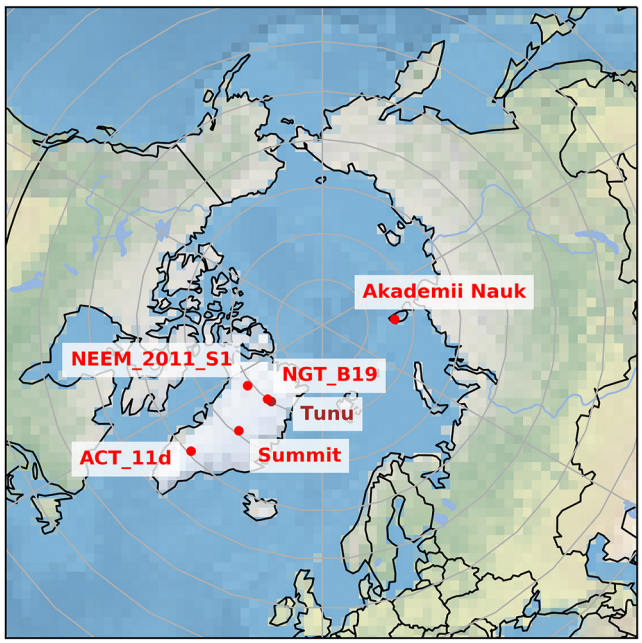

Figure 1. Location of the six ice cores used in this study.

located, in a global model for the first time. We present bromine records from six Arctic ice cores spanning from 1750–2007 CE and investigate their trends via statistical analysis. We used a global chemical transport model, GEOS-Chem, that includes snowpack reactive bromine emissions to examine the potential magnitude and spatial distribution of snowpack emissions relative to atmospheric deposition over the course of a full annual cycle, and evaluate the implications for preservation and interpretation of bromine records for these six ice cores.

2. Methods

2.1. Arctic Ice Cores

We present ice-core sodium, bromine, and acidity records from six Arctic ice cores covering the pre-industrial to present day transition (since 1750 CE), with five from the Greenland ice sheet and one from the Russian Arctic. Figure 1 shows the locations of the six ice-core sites. Table 1 summarizes the ice-core locations, age range, snow accumulation rates and references for previously published data. Here, we briefly describe the measurement techniques for the unpublished ice-core records, which include sodium, bromine, and acidity records from the Russian Arctic (Akademii Nauk), as well as bromine records from the five Greenland ice cores (ACT_11d, Summit_2010, NEEM_2011_S1, Tunu2013, NGT_B19).

A 724 m-long ice core was collected from the AN ice cap at Severnaya Zemlya in the central Russian Arctic from 1999 to 2001 (Fritzsche et al., 2002; Opel et al., 2013). Due to summertime surface melting, percolation into deeper layers and refreezing, the age scale was determined using an iterative approach based on annual layer counting using multi-parameter aerosol records constrained by absolutely dated reference horizons, called the DRI_Akademii_Nauk chronology, as described in McConnell et al. (2019). Uncertainty in the age scale was estimated to be less than 5 years. Tunu2013 (hereafter Tunu), North Greenland Traverse B19 (NGT_B19), NEEM_2011_S1, Summit_2010 (hereafter Summit), and ACT_11d are located on the Greenland ice sheet. Details of ice-core extraction and dating for these five ice cores can be found in previous publications (McConnell et al., 2019; Sigl et al., 2013).

For all ice cores, chemical analysis of elemental Na and elemental Br were conducted using continuous high resolution inductively coupled plasma mass spectrometry (HR-ICP-MS), at the Desert Research Institute (Maselli et al., 2017; McConnell et al., 2019), with an uncertainty of ±10%. Acidity (H^+) was directly measured continuously as described in Pasteris et al. (2012), with an error less than 5%.

Two metrics are normally used to assess the relative contribution of Br from sea salt and atmospheric processes, bromine excess (Br_{exc}) and bromine enrichment (Br_{enr}). The non-sea-salt Br concentration (Br_{exc}) is calculated as:

Table 1
Locations and Other Information for the Six Ice Cores Presented in This Study

Ice core	Latitude	Longitude	Elevation (m)	Snow accum. (kg m^{-2} yr^{-1})	Estimated age range (BCE/CE)	Elements and reference
Akademii Nauk (AN)	80.5°N	94.8°E	750	440	−200–1999	Br, Na (Spolaor et al., 2016a)
Tunu2013	78.0°N	33.9°W	2,105	108	275–2012	Acidity, Br and Na (Maselli et al., 2017)
NGT_B19	78.0°N	36.4°W	2,270	100	746–1993	Acidity and Na (Maselli et al., 2017)
NEEM_2011_S1	77.5°N	51.1°W	2,454	211	88–1999	Acidity and Na (Maselli et al., 2017)
Summit_2010	72.6°N	38.3°W	3,258	226	1743–2010	Acidity, Br and Na (Maselli et al., 2017)
ACT_11d	66.5°N	46.3°W	2,148	334	1161–2010	Acidity and Na (Maselli et al., 2017)

Note. References for previously published data are noted in the last column. See McConnell et al. (2019) for detailed ice core descriptions of Akademii Nauk, Tunu2013, NGT_B19, NEEM_2011_S1, Summit_2010, and ACT_11d.

$$[Br_{exc}] = [Br]_{ice\ core} - [ssNa]_{ice\ core} \times ([Br]/[Na])_{sea\ water} \quad (1)$$

where [X] represents mass concentrations in ng X g ice^{-1}, and $([Br]/[Na])_{sea\ water}$ is the sea water Br/Na mass ratio of 0.00624 (Millero et al., 2008). [ssNa] is calculated based on ice core calcium concentrations, as described in Maselli et al. (2017). The non-dimensional factor Br_{enr} is defined as the enrichment of Br relative to sea salt Br, and is calculated as:

$$[Br_{enr}] = [Br]_{ice\ core} / ([ssNa]_{ice\ core} \times ([Br]/[Na])_{sea\ water}) \quad (2)$$

A positive Br_{exc} is equivalent to $Br_{enr} > 1$, and a negative Br_{exc} is equivalent to $Br_{enr} < 1$. Br_{enr} will only be 0 if Br is under the detection limit. Br_{enr} is most often used as an ice core proxy because it is not influenced by changes in snow accumulation rates and absolute emissions of sea salt, and represents the degree of gas-aerosol re-partitioning including sea salt debromination (R8 –R9, with X = Br) (Spolaor et al., 2013a, 2013b). Trends in Br_{exc} will be more representative of trends in the concentration of Br_y in the atmosphere, facilitating comparison with atmospheric chemistry models.

2.2. Statistical Analysis of Ice-Core Observations

We use a recursive Bayesian change point algorithm based on dynamical programming (Ruggieri, 2013) to analyze the trends in ice core Br_{enr} and Br_{exc} records since pre-industrial time (1750 CE). Change points are defined as changes in the parameters of a regression model used to describe a climatic time series. Assuming a maximum of six change points in the ice core annual records since 1750 CE, a minimum separation time of 15 years between adjacent change points, and a linear fit in each identified regime, we sample 500 solutions independently from the posterior distribution, and calculate the best fit change point model (Ruggieri, 2013).

There are five parameters for the changepoint analysis, including the maximum number of change points allowed (k_{max}), the minimum distance between adjacent change points (d_{min}), and three hyperparameters for the prior distribution. We have chosen the three hyperparameters based on the recommendations from Ruggieri (2013), and conducted several sensitivity studies on choosing k_{max} and d_{min}. Tests with k_{max} ranging from 6 to 20, and d_{min} ranging from 5 to 20 show very similar results in changepoint identification, thus we show one of the results with $k_{max} = 6$ and $d_{min} = 15$.

2.3. Modeling Snowpack Halogen Chemistry

We use a 3-D global chemical transport model, GEOS-Chem (version 11-02d) (https://github.com/geoschem/geos-chem/tree/v11-02d-prelim), to examine post-depositional loss of snow bromine and its impact on ice-core bromine preservation. GEOS-Chem is driven by MERRA-2 assimilated meteorological observations from the Goddard Earth Observing System (Gelaro et al., 2017) and has detailed HO_x-NO_x-VOC-ozone-halogen-aerosol tropospheric chemistry, including comprehensive tropospheric multi-phase reactive halogen chemistry (Wang et al., 2019, 2021) and fully coupled stratospheric chemistry (Eastham et al., 2014). This model also incorporates blowing snow-sourced SSA emissions (Huang & Jaeglé, 2017). Gas phase and heterogeneous bromine chemistry are described in previous papers (Chen et al., 2017; Sherwen et al., 2016; Wang et al., 2021). Sea-salt aerosol debromination occurs on both open ocean and blowing snow sourced SSA (Huang et al., 2020). Gases and water-soluble aerosols are wet deposited in GEOS-Chem based on scheme described in Amos et al. (2012) and Liu et al. (2001), respectively. Dry deposition is based on the resistance-in-series scheme introduced in Wesely (1989) as implemented by Wang et al. (1998). Among Br_y species, Br_2, HOBr, HBr, BrCl, IBr and aerosol bromide are both wet and dry deposited, and $BrNO_3$ is dry deposited only. We updated the O_3 dry deposition scheme onto snow and ice surface, such that the dry deposition velocity is about 0.01 cm s^{-1}, consistent with observations (Simpson et al., 2007a) and assumptions made in Toyota et al. (2011). We run all simulations at $4 \times 5°$ horizontal resolution and 72 vertical levels up to 0.1 hPa for 1 year using 2007 meteorology, after spinning up the model for 1 year. An additional sensitivity simulation was performed using 2008 meteorology. Coal combustion and leaded gasoline emitted bromine are not included in the model, because the former suffers large uncertainty (Lee et al., 2018) and is considered a minor source, and the latter is not important in present day (Lammel et al., 2002; Thomas et al., 1997).

Bromine from snowpack is emitted into the lowest level of the model. Modeling snow chemistry emissions from the snow surface skin layer (approximately 1 mm at the top, Erbland et al., 2013) adopts the framework from

Table 2
Comparison of Key Model Settings Conceived by Toyota et al. (2011) and the Three Model Simulations (mToyota, SURF, and DEEP) in This Study

Model simulation	Toyota et al. (2011)	mToyota (Modified Toyota)	SURF (surface production only)	DEEP (surface and deep production)
Snow Bromide Concentration	Constant Br^-: infinite Br^- on FYI Br^- on MYI and LS only replenished by dry deposition of HBr	Track surface snow Br^-: Snow Br^- = initial + HBr dry deposition + sea salt Br^- dry deposition—released Br_2	Track surface snow Br^-	Track surface snow Br^-, unlimited deeper snow bromide
Surface snow production	100% molar yield of Br_2/BrCl on HOBr and $BrNO_3$ deposition; 0.1% molar yield on O_3 deposition	Same as Toyota et al. (2011)	Same as Toyota et al. (2011)	Same as Toyota et al. (2011)
Deeper snow production	Implicitly represented: 7.5% molar yield of Br_2 on O_3 deposition under sunlit conditions	Same as Toyota et al. (2011)	No deep production	$F_{Br2} = F_{1Dmax} \times \cos(SZA)$
Additional threshold	Temperature below −10, −15, or −20°C	Temperature below 0°C. Snow depth > 10 cm for land snow	Temperature below 0°C. Snow depth > 10 cm for land snow	Temperature below 0°C. Snow depth > 10 cm for land snow albedo > 0.7

Toyota et al. (2011), with several updates to represent surface snow production of BrX at inland locations as described below. In Toyota et al. (2011), reactive halogen release from the surface snowpack is driven by deposition of HOBr, $BrNO_3$, and O_3 with molar yields dependent on snow type and availability of snow halides. Toyota et al. (2011) assumed unlimited snow bromide for first-year sea ice, limited bromide sourced from dry deposition of HBr and infinite chloride for multi-year sea ice, and no snow halides for land snow. Dry deposited HOBr and $BrNO_3$ are fully converted to BrX based on availability of snow halides. For sea ice regions, once snow bromide is depleted, dry deposited HOBr and $BrNO_3$ react with snow chloride to form BrCl, with a molar yield of 100%. Br_2 formation through reactive uptake of O_3 on surface snow is represented by converting the O_3 deposition flux on surface snow into the emission flux of Br_2, with a molar yield of 0.1% under dark conditions and 7.5% under sunlit conditions. The value 0.1% represents Br_2 formed via ozone uptake on frozen seawater in the dark (Oum et al., 1998; Wren et al., 2010), while 7.5% is the adjusted value based on the comparison between the model and hourly measurements of surface ozone at the coastal sites of Alert, Barrow, and Zeppelin in April 2001 (Toyota et al., 2011). This empirically adjusted molar yield for sunlit conditions (7.5%) is used in the GEM-AQ model (Toyota et al., 2011) to account for the deeper snow production of reactive bromine, which is highly dependent on solar radiation. This molar yield also introduces some uncertainty when applied to inland sites like Greenland, since its value is based on coastal observations.

Table 2 describes three model simulations performed here. All three simulations account for surface recycling of bromine from deposition of HOBr and $BrNO_3$ to form Br_2 using a molar yield of unity, and from deposition of O_3 using a molar yield of 0.1% to form Br_2. The treatment of surface recycling is similar to Toyota et al. (2011), except that we explicitly track surface snow bromide concentration for all snow types, instead of assuming unchanging bromide content based on snow types. Surface recycling of reactive bromine is limited by the availability of reactive bromide in the snow. Surface snow bromide originates from dry deposition of HBr and SSA bromide, and is lost by chemical production of Br_2 (R6, R7, and R9). In contrast, Toyota et al. (2011) assumed only dry deposition of HBr as a source of snow bromide.

We assume fresh snowfall contains no reactive bromide, effectively assuming that wet deposited bromide is trapped in the frozen snow grain and not available for surface reactions (Domine et al., 2013). Processes such as snow sublimation and re-deposition may alter the location of bromide within the snow grain over time, likely rendering this an underestimation of snow bromide on the surface of snow grains that is available for surface chemical reactions. On the other hand, temperature gradient snow metamorphism is shown to facilitate the burial of bromide, resulting in the absence of bromide from the air–ice interface (Edebeli et al., 2020). We also do not consider the upward migration of bromide in snow from sea ice as a replenishing source for surface snow bromide, which may result in an underestimate of snow bromide concentrations over sea ice (Domine et al., 2004). However, upward migration is not a source of bromide in inland snow, where ice cores are drilled, which is the focus of this study. The model simulation that contains only surface snow recycling source is referred to as SURF.

For the other model simulations, we included two representations of deeper snow production in addition to surface recycling. In the "mToyota" simulation, we increase the molar yield of Br_2 production from ozone deposition to 7.5% under sunlit conditions to account for deeper snow production as in Toyota et al. (2011). Although deeper snow production is unlikely to be directly influenced by ozone deposition to the skin layer, this parameterization was shown to provide good agreement with BrO observations in springtime at specific coastal locations and time periods in the Arctic spring time.

In the "DEEP" simulation, we effectively assume that ozone and OH production deeper in the snow originates from the photolysis of snow nitrate and H_2O_2 (e.g., Grannas

et al., 2007), and that oxidants produced in the SIA will react with bromide in the deeper snow to form HOBr (R6 and R7) (Thomas et al., 2011; Toyota et al., 2014). The production of HOBr in SIA is necessary for in-snow bromine production of Br_2 (R9). Since photolysis of snow nitrate and H_2O_2 is driven by sunlight, we scale Br_2 release from deeper snow to the SZA with a maximum flux based on order-of-magnitude estimates from previous 1D snow photochemistry modeling studies (Toyota et al., 2014), as shown in Equation 3.

$$F_{\mathrm{Br2}} = F_{\mathrm{1Dmax}} \times \cos(\mathrm{SZA}) \tag{3}$$

where F_{Br2} is the Br_2 emission flux, F_{1Dmax} is the maximum Br_2 emission flux from previous 1D model simulations, and SZA is the solar zenith angle. We chose F_{1Dmax} to be 1×10^8 atom Br cm^{-2} s^{-1} (8.64×10^{12} atom Br cm^{-2} day^{-1}) based on Toyota et al. (2014), which is roughly the daily maximum upward flux of total inorganic gaseous bromine below the snow skin layer in March. This value is similar in magnitude to that of Thomas et al. (2011), which used a 1D model to simulate snowpack bromine emissions at Summit Greenland in June 2008. Note that F_{1Dmax} is 1 order of magnitude smaller than the measured emission flux reported in February at Utqiagvik, Alaska (Custard et al., 2017), and the 1D model (Toyota et al., 2014) assumes the source of snow bromide to be only from atmospheric deposition. Thus, the DEEP simulation is anticipated to underestimate coastal snow bromine emissions by at least an order of magnitude. We added a temperature and albedo threshold to reflect the impact of surface melting on snowpack bromine release. When albedo is below 0.7 (Custard et al., 2017; McConnell et al., 2017) or surface temperature are greater than 0°C (Burd et al., 2017), the deeper snow production of bromine is ceased. In comparison, Toyota et al. (2011) allows snowpack bromine emissions only when temperature is below a "critical temperature," which varies between −10°C and −20°C in their sensitivity studies. Following Swanson et al. (2022), we adopt a threshold of snow depth of 10 cm over which snowpack bromine release is allowed for land snow regions, preventing excessive bromine production in lower-latitude snow-covered regions. We assume bromine content is not a limiting factor for deeper snow production, similar to Toyota et al. (2014), because we are unable to track snow bromide in deep snow over time without an explicit 3D snow module. Unlike surface snow, bromide in deeper snow cannot be replenished through atmospheric deposition, so this assumption may lead to a model overestimate of bromine release from deeper snow at inland locations. We do not explicitly consider the effect of wind pumping and snow acidity in this simplified scheme, both of which facilitate snow bromine release (Custard et al., 2017; McConnell et al., 2017).

Total snowpack bromine emission flux (F_{eBr}) is the sum of Br_2 and BrCl emissions from the surface skin layer, and the Br_2 emissions from deeper snow (F_{Br2}). Post-depositional loss of bromine is evaluated in the model by comparing total surface deposition fluxes to snow emissions fluxes (Equation 4):

$$R_{\mathrm{loss}} = \frac{F_{\mathrm{eBr}}}{F_{\mathrm{dBr}}} \times 100 \tag{4}$$

where R_{loss} is the post-depositional loss of bromine in percentage, F_{eBr} is the total snowpack emission flux of bromine including Br_2 and BrCl emissions, and F_{dBr} is the total deposition flux including wet and dry deposition of HBr and SSA bromide.

We do not include snow chemistry for molecular chlorine (Cl_2) in this study. Cl_2 was not observed above the instrument detection limit of 2 ppt during field campaigns in Alert, Canada (Foster et al., 2001; Spicer et al., 2002), or in the snow chamber experiment in Utqiagvik, Alaska (Pratt et al., 2013), but was detected at up to 400 ppt in spring at Utqiagvik, AK (Custard et al., 2016; Liao et al., 2014). Cl_2 production is likely limited by the snow Cl^- availability, since snow temperature is likely below the eutectic point (251K) for the formation of $NaCl{\bullet}2H_2O$ (Koop et al., 2000). Studies report different ranges for molecular chlorine emission flux from snowpack, but almost all observation-based calculations show that Cl_2 fluxes and concentration are much lower than Br_2. Compared to the chlorine deposition flux in polar regions (10^{13} –10^{14} molecules cm^{-2} s^{-1}) (Zhai et al., 2021), the snowpack emission of Cl_2 is at least four orders of magnitude smaller, thus is unlikely to represent a significant loss process for ice core chlorine.

3. Results

3.1. Ice-Core Bromine Trend Analysis

Figure 2 shows bromine records from the six Arctic ice cores. The average total bromine concentrations in AN ice core are 4–10 times higher than those for the Greenland ice cores. This is likely due to the proximity of AN to open ocean and the relatively low elevation compared to inland Greenland, as indicated by the average sodium

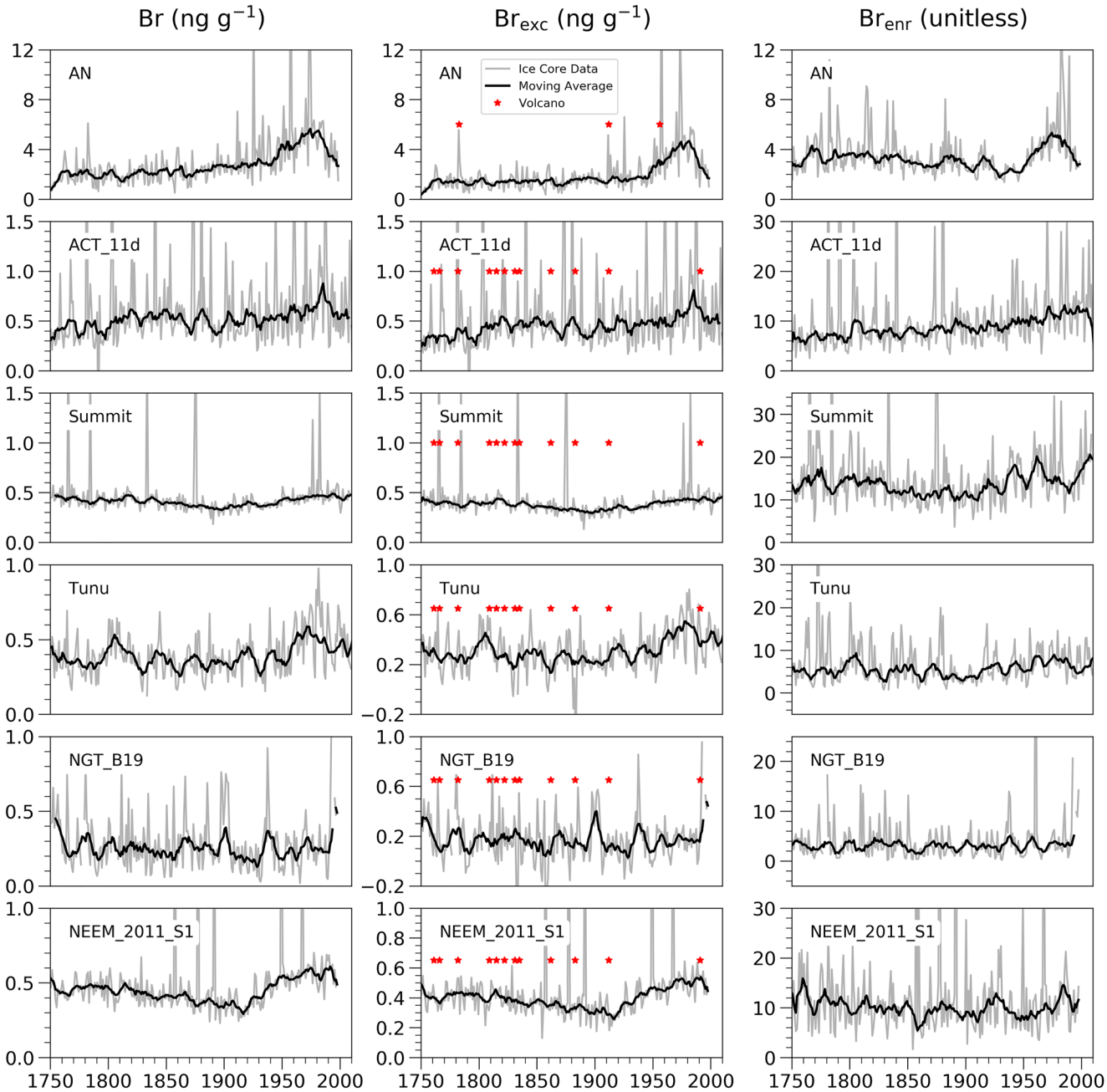

Figure 2. Total bromine concentration (left), Br_{exc} (middle), and Br_{enr} (right) in the Akademii Nauk (AN), ACT_11d, Summit, Tunu, NGT_B19, and NEEM_2011_S1 ice cores. Gray lines are the measured annual ice core concentrations (total bromine) or calculations (Br_{exc} and Br_{enr}), and black lines are the 9-year running average, with outliers outside of 1.5 × IQR (interquartile range) removed. Red stars mark the large and moderate volcanic years identified in previous studies (Opel et al. (2013) for AN and Cole-Dai et al. (2013) and Sigl et al. (2013) for Greenland ice cores, see also Figure S1 in Supporting Information S1).

concentrations at AN that are 8–28 times higher than those for Greenland locations (Figure S1 in Supporting Information S1). AN also has 3–11 times higher Br_{exc} concentrations compared to the Greenland ice cores. Br_{enr} values at AN are smaller (0.2–0.8 times) compared to Greenland ice cores. This suggests that the extent of aerosol debromination at AN is not as extensive as in inland Greenland. Since AN is located closer to the open-ocean and sea-ice sea salt emission sources compared to the Greenland sites, it will experience more bromine-depleted coarse mode sea salt deposition. In contrast, only gas phase bromine and accumulation mode sea salt, which are bromine-enriched and have a longer lifetime, are transported the longer distance from sea salt source regions to the Greenland sites, resulting in higher Br_{enr} (Domine et al., 2004; Nandan et al., 2017; Hara et al. (2002)).

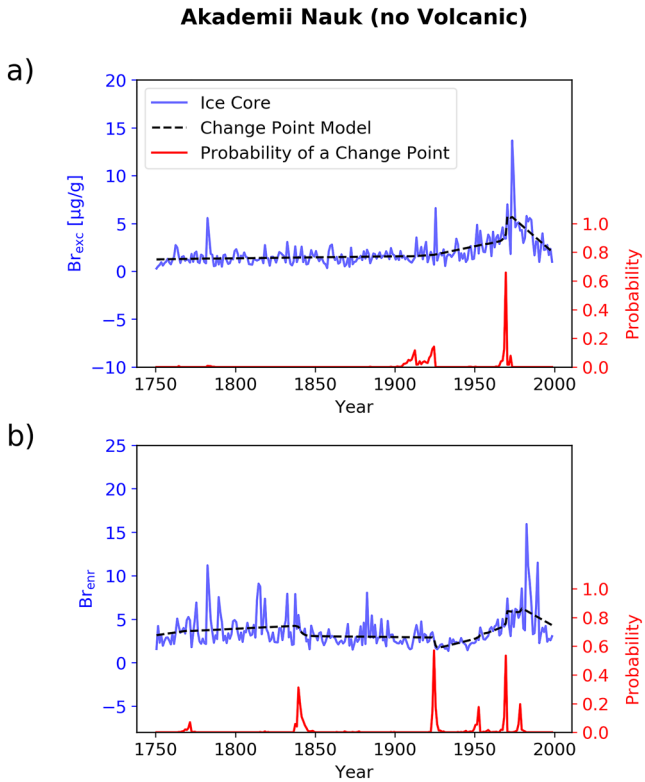

Figure 3. Ice-core records and trend analysis of (a) Br_{exc} and (b) Br_{enr} since year 1750 from the Akademii Nauk ice core. Blue lines are ice core Br_{exc} and Br_{enr} values calculated based on ice core measurements of sea-salt sodium and bromine, with previously identified volcanic years removed (Opel et al., 2013). Dashed black lines are the model predicted trends by the Bayesian Change Point algorithm. The heights of red spikes at the bottom of each panel indicate the probability of a potential change point. Tall, narrow spikes suggest relative certainty in the timing of a change point, whereas shorter and wider spikes suggest more uncertainty. No spikes are visible if no change points are identified by any of the 500 sampled solutions. Similar analysis for other ice core locations are in Figures S2 and S3 in Supporting Information S1.

Change point analysis shows that of the six ice cores, only AN has significant trends in Br_{exc} and Br_{enr} since the pre-industrial (Text S2, Figures S2, and S3 in Supporting Information S1). Figure 3 shows the results of the change point analysis for the AN core, with volcanic years removed (Opel et al., 2013). AN Br_{exc} remained at a relatively stable concentration of 1.5 ± 0.8 ng·g^{-1} from 1750 to 1940, showed a 3.7-fold increase from 1940 to 1975 (5.6 ± 3.5 ng·g^{-1}), and decreased afterward by −57% (2.4 ± 0.9 ng·g^{-1}). AN Br_{enr} before 1850 had an average value of 3.3 ± 1.5. After 1940, AN Br_{enr} increased 1.6-fold until 1975 (5.3 ± 1.5), and decreased by −21% afterward (4.2 ± 2.7).

The presence or absence of ice core bromine trends in and of themselves is not necessarily indicative of the degree of bromine preservation, at least in part because the source regions for each ice core location may differ from one another. Previous studies have attributed ice core bromine trends to changes in sea ice extent (Spolaor et al., 2013a, 2013b, 2016a, 2016b; Maffezzoli et al., 2021), atmospheric acidity (Maselli et al., 2017), and anthropogenic bromine emissions from leaded gasoline (Legrand et al., 2021). Figure S4 in Supporting Information S1 shows the calculated 5-day back trajectory probability from the HYSPLIT model for AN, and readers are referred to Figure S2 in Zhai et al. (2021) for 5-day back trajectory plots for the Greenland ice core locations. Major sea ice source regions (>60% regional contribution) for the Greenland ice cores are the Greenland Sea, Baffin Bay and Labrador Sea, while for AN are the Laptev Sea, Kara Sea, Barents Sea, and the Arctic Ocean. Sea ice extent has been declining across the Arctic since 1980 (Brennan & Hakim, 2021), but sea ice extent in the Russian Arctic, especially in Barents Sea, has been decreasing faster than the source regions for Greenland ice cores (Comiso et al., 2017). Major source regions of potential anthropogenic emissions are eastern North America and Northwestern Europe for Greenland ice cores, and Russia and Eastern Europe for AN.

Spolaor et al. (2016a) found that ice core Br_{exc} concentration in AN was positively correlated ($r = 0.44$, p-value $= 0.02$) with the Laptev Sea spring sea ice extent since 1979. Although satellite observations of sea ice are not available prior to 1979, sea ice reconstructions suggest small increases in sea ice extent after about 1940 until about 1980 in the Russian Arctic, East Greenland Sea, and Baffin Bay (Brennan & Hakim, 2021; Mahoney et al., 2008), qualitatively consistent with the increasing trends in AN Br_{enr} and Br_{exc} from 1940 to the 1970s (Figures 2 and 3). If Greenland ice core bromine is influenced by sea ice extent, then we would also expect to see an increase in Br_{enr} and Br_{exc} between 1940 and the 1970s followed by a more rapid decrease since 1979, which is not observed (Figures S2 and S3 in Supporting Information S1).

Assuming that ice core methanesulfonic acid (MSA) is a sea ice proxy, Maselli et al. (2017) calculated sea-ice sourced bromine based on the linear regression of ice core MSA and bromine during 1750–1880 CE, and attributed trends in non-sea ice bromine in Greenland ice cores (Summit and Tunu) after the mid-20th century to changes in atmospheric acidity, which is known to facilitate aerosol debromination reactions. Measured acidity is similar in all six ice cores, with an increasing trend beginning in the 1940s followed by a decreasing trend after the 1970s (Figure S1 in Supporting Information S1). These trends in acidity are similar to the observed trends in Br_{exc} and Br_{enr} in the AN core. The existence of acidity trends combined with the lack of bromine trends over the same time period in the Greenland ice cores suggest either that acidity is not influencing Greenland ice core bromine trends, or that acidity-driven trends in bromine are not preserved in the Greenland ice cores.

Legrand et al. (2021) found that anthropogenic emissions from leaded gasoline, which is the largest historical anthropogenic source of bromine, is the major driver of summertime ice core bromine trends from the Col du Dome (CDD) ice core in French Alps. Trends in leaded gasoline usage are similar to the acidity trends (Figure S1 in Supporting Information S1), increasing from the 1940s to 1970s and decreasing since the 1970s in North America, Europe, and Russia (Thomas et al., 1997), which are the major source regions for the Greenland ice

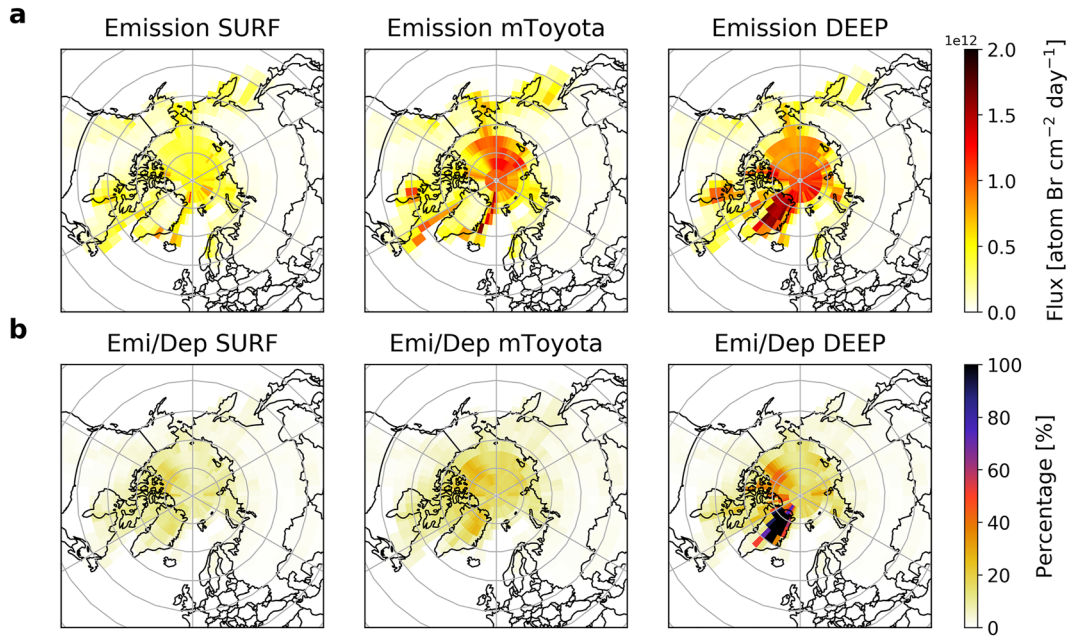

Figure 4. Simulated Arctic spatial distribution of annual mean (a) snowpack emission fluxes of bromine (Br_2+BrCl), and (b) post-depositional loss calculated as the percentage of snowpack bromine emission fluxes (Br_2+BrCl) divided by total bromine deposition (dry + wet) from the three simulations, SURF, mToyota, and DEEP.

cores and AN (Figure S4 in Supporting Information S1). We note that sea ice extent, atmospheric acidity, and anthropogenic emissions of bromine all increased between the 1940s and the 1970s and declined after the 1970s, but only the AN core shows corresponding trends in Br_{exc} and Br_{enr} over this time period. The lack of significant trends in Greenland ice core bromine metrics may be due to poor preservation of bromine in snow and ice at these locations.

3.2. Modeled Snowpack Reactive Bromine Release

Figure 4a shows the model simulated annual mean snowpack bromine emission fluxes in the Arctic region. The model likely underestimates the total Br_2 emission flux at coastal sites for all three model simulations, based on comparisons of the modeled emissions fluxes and prior field measurements. For example, at Utqiagvik in February, the model calculates a monthly average bromine emission flux of 6.3–9.1 × 10^{10} atom Br cm^{-2} day^{-1} for the three simulations, about three orders of magnitude lower than those reported in Custard et al. (2017) from February 14th and 16t 2014 (0.7–12 × 10^8 molecules cm^{-2} s^{-1}, or 1.2–21 × 10^{13} atom Br cm^{-2} day^{-1}). The modeled snowpack bromine emission fluxes in the sea ice regions from DEEP and mToyota are also about 1 order of magnitude smaller than reported in previous 3D models for Arctic conditions in April (Swanson et al., 2022; Toyota et al., 2011). The underestimation in coastal regions is due to our conservative assumption of surface snow bromide content, which lacks replenishment from upward migration from sea ice (Domine et al., 2004; Nandan et al., 2017). This suggests that upward migration of bromide through the snow layer from sea ice may be important for reactive bromine emissions and ODEs in the coastal Arctic.

Figure 4b shows the model simulated annual post-depositional loss of snow bromine in the Arctic region, calculated by comparing bromine surface deposition with snow emissions (Equation 4). The modeled maximum annual mean post-depositional loss across the Arctic is 26%, 50%, and >100% from SURF, mToyota, and DEEP simulations, respectively. In DEEP, post-depositional loss >100% is calculated only in inland central and northern Greenland, where most of the ice cores are drilled, suggesting that DEEP overestimates snowpack bromine emissions at these sites.

Table 3 shows the deposition and emission fluxes between the snowpack and atmosphere for the six ice core locations from the SURF and DEEP simulations. The calculations for mToyota are in between these two simulations and are shown in Supporting Information S1 (Table S1). SURF simulation predicts similar post-depositional

Table 3
Annual Mean Snowpack-Air Exchange Fluxes of Total Bromine (Total Deposition, Emission, Net Upward Flux, and Post-Depositional Loss) at the Six Ice Core Locations Calculated From the SURF and DEEP Simulations

Ice core	Total deposition [$\times 10^{11}$ atom Br cm^{-2} day^{-1}]	Emission (Br_2+BrCl) [$\times 10^{11}$ atom Br cm^{-2} day^{-1}]	Net upward flux [$\times 10^{11}$ atom Br cm^{-2} day^{-1}]	Post-depositional loss (Emission/deposition)
AN	33–38	5.5–12	−28 to −26	17%–32%
Summit_2010	4.3–8.6	0.6–15	−3.7 to +6.4	14%–172%
Tunu2013	4.7–11	0.6–15	−4.1 to +4.0	13%–142%
ACT_11d	22–26	2.0–13	−2.0 to −1.3	9%–51%
NEEM_2011_S1	7.2–13	0.7–15	−6.5 to +2.0	10%–113%
NGT_B19	4.7–11	0.6–15	−4.1 to +4.0	13%–142%

Note. The lower and higher ends of the range are values calculated from the SURF and DEEP, respectively.

loss (9–17%) across all six ice-core locations, suggesting that factors such as snow accumulation rate, elevation, and distance from the coast have minimal impact on bromine loss from surface recycling. The largest snowpack bromine emission flux in the SURF simulation is 5.5×10^{11} atom Br cm^{-2} day^{-1} at AN, twice the value at ACT_11d, and 8–9 times of the values at northern Greenland ice-core sites. The relatively large emissions flux from surface recycling at AN and ACT_11d is driven by larger HBr and sea salt Br^- deposition flux at these two locations. Compared to the observed annual mean ice core bromine concentrations, SURF simulated snow bromide is about 2–8 times higher (Table S2 in Supporting Information S1), suggesting that loss from deeper snow production is needed to explain the observed snow bromine concentrations in ice cores. The mToyota simulation, which assumes a higher yield of Br_2 from O_3 deposition during sunlit periods compared to SURF, predicts higher emission fluxes and therefore slightly higher post-depositional loss of 13–25% across all six ice core locations.

The DEEP simulation predicts much higher post-depositional loss everywhere compared to the other two simulations, especially in inland Greenland (Figure 4). In DEEP, total annual snow emissions are larger than total annual deposition at all ice-core sites except AN and ACT_11d. Since deposition is the only source of snow bromine at inland locations, this is not physically possible, demonstrating that our assumptions of snow emissions in DEEP constrained by 1D model studies in coastal spring and summertime inland sites result in an overestimate of annual snow bromine emissions. However, even with the overestimated bromine emissions from deeper snow in the model, the DEEP simulation still predicts significant (68%) preservation of snow bromine at the AN location, consistent with the observation that only this ice core has significant trends in Br_{exc} and Br_{enr}. The four northern Greenland ice cores (Summit, Tunu, NEEM_2011_S1, and NGT_B19) have very similar emission fluxes, since deeper production in the model is determined by F_{1Dmax} scaled by the cosine of SZA. Emissions at AN and ACT_11d are slightly lower due to summertime surface melting in the modeled year (2007), which shuts down deeper production in the model. The comparison between SURF and DEEP shows that bromine loss within the snow photic zone but beneath the snow surface layer dominates total loss from the snowpack in the model in the DEEP simulation, in agreement with Toyota et al. (2014).

Figure 5a shows modeled seasonality in snowpack bromine emissions at the six ice-core sites for each model simulation. Monthly mean bromine emission fluxes range from 1×10^9 to 1×10^{12} atom Br cm^{-2} day^{-1} at all sites throughout the year from surface recycling only (SURF). Loss from surface recycling is largely driven by the seasonality of dry deposition of total bromine (Br_y + sea salt Br^-) and ozone (Figure S5 in Supporting Information S1). The mToyota simulation predicts higher emission fluxes in April at AN but similar emission fluxes with SURF in other months and locations, mainly driven by the seasonality in the deposition flux of ozone, the availability of solar radiation, and snow Br^- concentrations. In April, the high values of dry deposition fluxes of ozone and bromine (thus snow Br^-) accelerates snow Br^- oxidation by ozone. Whereas in May, even though ozone deposition remains large, limited snow Br^- hinders further production of bromine from the snowpack.

The DEEP simulation results in much higher maximum emission fluxes compared to SURF and mToyota, and are similar in seasonality and magnitude (with a maximum of $\sim 4 \times 10^{12}$ atom Br cm^{-2} day^{-1}) among the ice-core sites since they are limited by the value of F_{1Dmax} (8.64×10^{12} atom Br cm^{-2} day^{-1}) scaled to the SZA. Peak

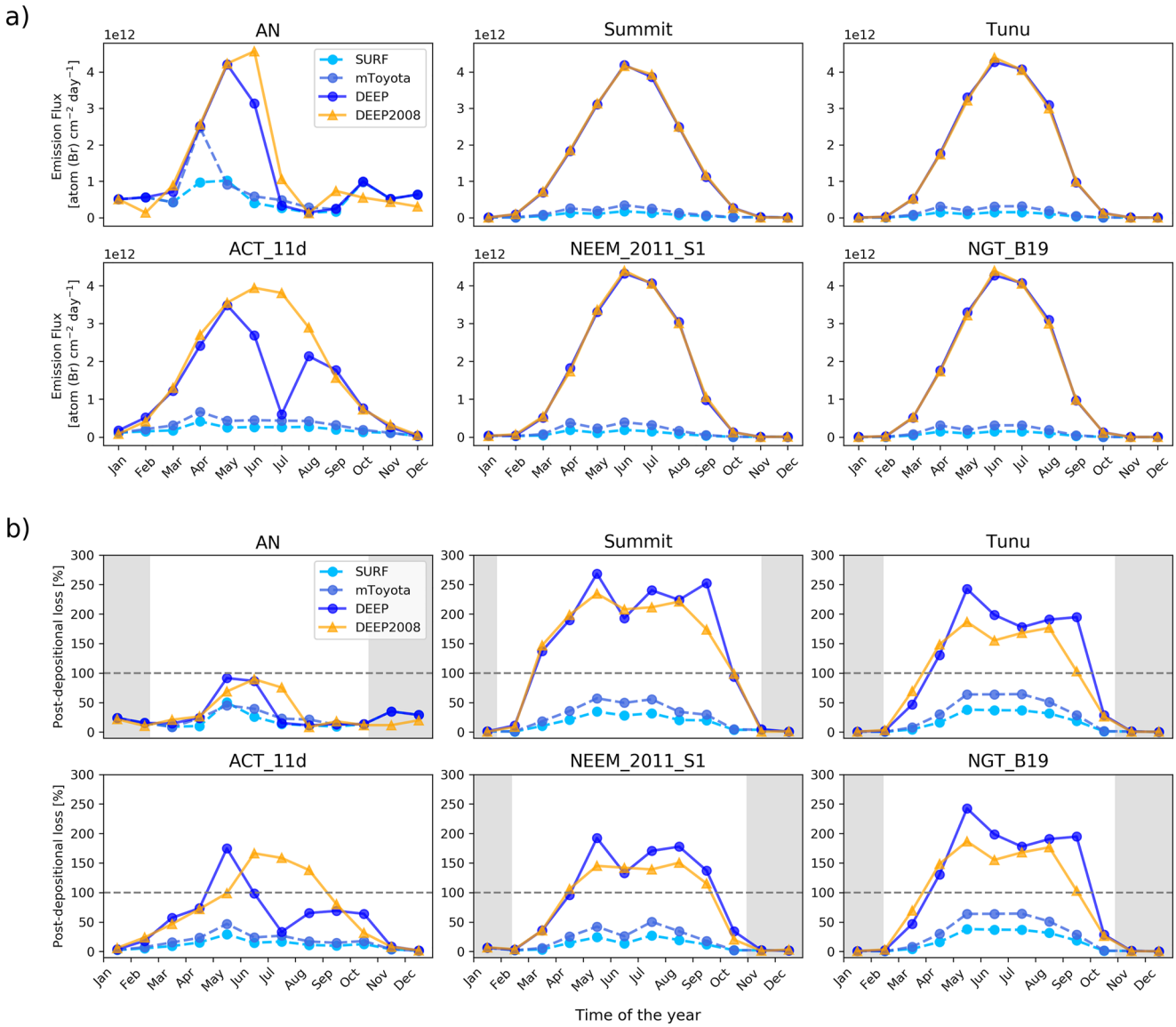

Figure 5. Modeled monthly mean snowpack (a) total bromine (Br_2 + BrCl) emission fluxes and (b) post-depositional loss in percentage at the six ice-core sites from the three simulations for year 2007: SURF, mToyota, and DEEP, and the DEEP simulation for year 2008. Dashed gray lines mark 100% loss, above which there is mass imbalance (i.e., total emission larger than total deposition). Gray area is the dark period in polar winter.

monthly emissions at all sites except for AN and ACT_11d are predicted in June following the seasonality of the SZA. Surface melting at AN and ACT_11d in summer shuts down the deeper snow bromine production, resulting in late spring peak (May) in snowpack bromine release at these two sites. For AN, surface melting occurs in summer and autumn (June–October in year 2007) which explains the low bromine emission fluxes beginning in June until the next polar sunrise. At ACT_11d, surface melting and the shutdown of deep snow photochemical reactions occurs from June to early August in year 2007 (Figure S6 in Supporting Information S1), and similar emission fluxes to those of the other Greenland ice cores are found in other months.

Annual variations in summertime temperature and albedo have a large impact on the seasonality of snowpack bromine emissions at AN and ACT_11d. A sensitivity model simulation of the DEEP parameterization for year 2008 shows that the emission flux of bromine peaked in June at AN and ACT_11d for year 2008, instead of May for the year 2007 (Figure 5a). For AN, surface melting does not start until July 2008 (Figure S6 in Supporting Information S1). For ACT_11d, the albedo remained above 0.7 throughout summer 2008 (Figure S6 in Supporting Information S1), resulting in a bell-shaped seasonality in snowpack bromine release similar to other

Greenland sites. Comparison between year 2007 and 2008 shows that, lower summertime temperature and later melt onset date postponed the peak emission time at AN and ACT_11d from late spring (May) to early summer (June), and increased the post-depositional loss from 32% in 2007 to 35% in 2008 for AN, and 51% in 2007 to 68% in 2008 for ACT_11d.

Figure 5b shows the monthly average percentage post-depositional loss at each ice-core site calculated according to Equation 4. In our deep snow bromine production mechanism, there is no limit on available snow bromide that can sustain the photochemistry to produce molecular bromine, therefore we are essentially assuming infinite supply of snow bromide in the snow photic zone below the skin layer. As a result, most Greenland ice cores have mass imbalance (total bromine emission fluxes exceeding total bromine deposition fluxes) lasting for 5–7 months. This is not possible, since the photochemically available snow bromide will be depleted at some point, and will not sustain further bromine production from deeper snowpack due to lack of replenishment. At that point, surface recycling should be the only mechanism that is producing bromine from the snowpack.

Satellite observations show that BrO VCDs peak in coastal Artic spring (Bougoudis et al., 2020), suggesting factors other than SZA and actinic flux as drivers of deeper snow reactive bromine production. We speculate that photochemically reactive bromide deeper in the snow is depleted at some point and becomes a limiting factor for snow bromine emissions during the sunlit season. Because snow bromide concentrations are always greater than zero in Arctic ice cores (Figure 2), bromide that is subject to photochemical or reactive loss may represent only a fraction of total bromide in snow and ice. It is also possible that precursors to oxidant formation in the snowpack such as photolabile nitrate and H_2O_2 also become depleted and limit the production of oxidants and thus bromine loss deeper in the snowpack over the course of the sunlit season.

Our model underestimates the source of Br_y in the sea ice region, and this underestimate would mostly impact the transport and deposition of bromine to the AN core due to its closer proximity to sea ice compared to the Greenland ice cores. The model's mass imbalance in Greenland may also be partially explained by underestimated source of Br_y to the atmosphere. The model does not include anthropogenic bromine emissions from coal combustion (Lee et al., 2018). Both Greenland and AN ice cores show trends in anthropogenic emissions of acidity (Figure S1 in Supporting Information S1), showing that emissions from anthropogenic source regions influence Arctic ice core records. Our model for deep snow production of Br_2 is a simplified parameterization that is solely based on SZA and independent of snowpack bromine concentrations. The lack of anthropogenic emissions of bromine species leads to an underestimate of total deposition, which in turn could cause an overestimate of post-depositional loss due to the low bias in the denominator (deposition flux).

The only available ground-based observations of near surface bromine species in an inland Arctic region were during May–June in 2007 and June–July in 2008. Stutz et al. (2011) observed a typical BrO mixing ratio of 1–3 pmol mol^{-1} and a maximum of up to 5 pmol mol^{-1} at Summit, Greenland using long-path differential optical absorption spectroscopy (LP-DOAS), which was shown to have excellent agreement with BrO measured by chemical ionization mass spectrometry (Liao et al., 2011a, 2011b). During the same campaign, Dibb et al. (2010) used Mist Chamber-Ion Chromatography to measure soluble Br^- concentrations, with soluble Br^- determined to be $[Br^-] = 0.9[Br_2] + 1.0[HOBr] + 0.4[BrO] + 0.95[HBr]$ (in mol) (Liao et al., 2012), and reported mean soluble Br^- values of 0.7 ppt for 2007 and 0.3 ppt for 2008 (Dibb et al., 2010). Comparison of LP-DOAS BrO and mist-chamber soluble bromide observations shows that the observed BrO alone can exceed soluble bromide observations, even when accounting for the factor of 0.4 contribution of BrO to the mist-chamber observations. The observed LP-DOAS BrO of 1–3 ppt suggest that BrO would contribute typically 0.4–1.2 ppt to the mist-chamber soluble bromide. This exceeds the mean of the observed mist-chamber soluble bromide (0.7 ppt).

The DEEP modeled hourly surface BrO mixing ratio shows good agreement with the observed BrO from LP-DOAS (Figure 6), but overestimates soluble Br^- (Figure S7 in Supporting Information S1). Modeled afternoon boundary layer height at Summit during the campaign seasons is 267–357 m, similar to the daytime boundary layer height estimated in Thomas et al. (2011) (20–30 m at night, and 200–300 m during daytime). The modeled BrO concentrations in the DEEP simulation are between 0 and 4 ppt, with an average of 1.2 ppt for 2007 and 0.9 ppt for 2008, which is similar to those observed by Stutz et al. (2011). However, the modeled soluble Br^- has an average of 3.1 ppt for 2007 season and 3.7 ppt for 2008 season from the DEEP scheme, more than a factor of 3 higher than those observed by Dibb et al. (2010). As shown in Fig.S7, the major components for soluble $Br^-$are HOBr and HBr. BrO in the SURF simulation is 0.2 and 0.1 pmol mol^{-1} for 2007 and 2008 season, respectively (Figure 6), about 1 order of magnitude lower than Stutz et al. (2011) reported. However, SURF simulated

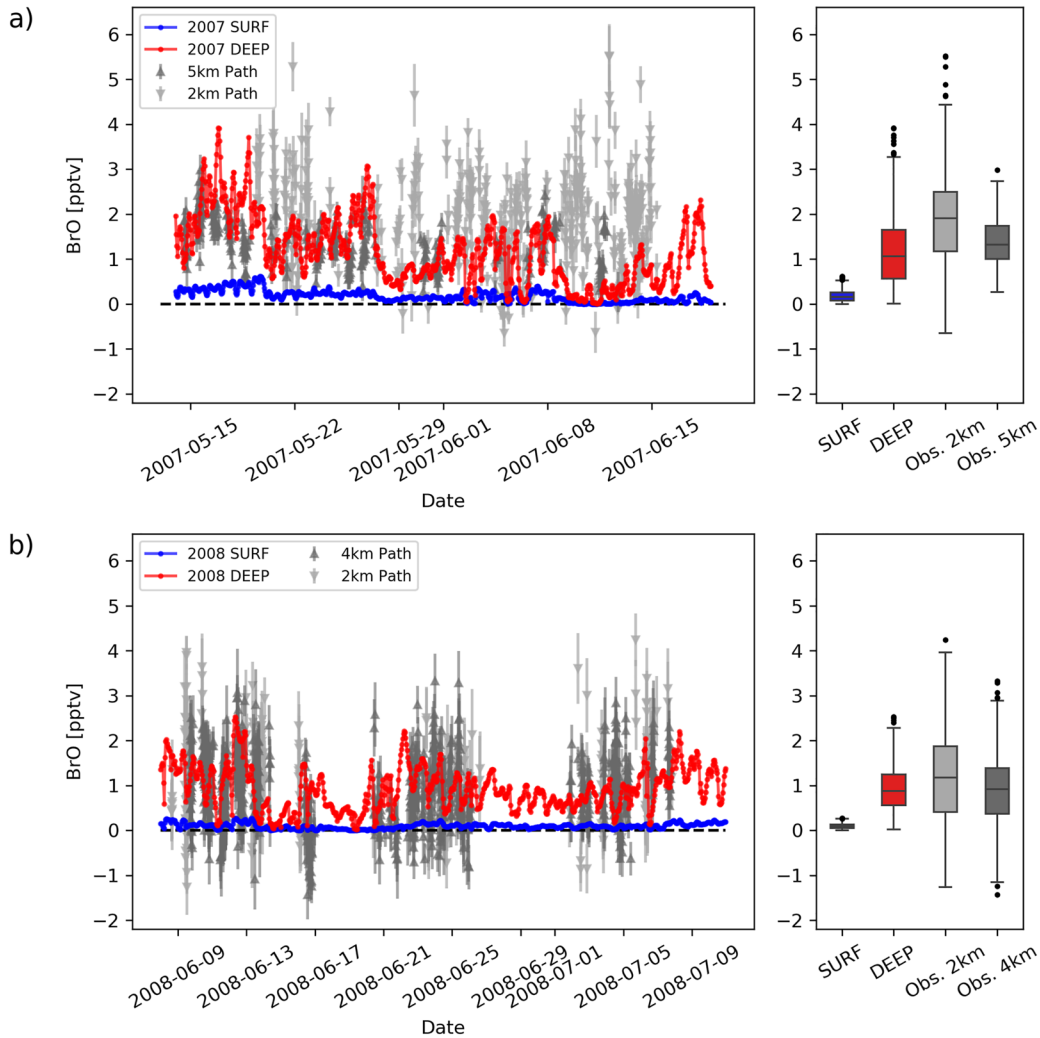

Figure 6. Comparison between the modeled hourly surface BrO concentrations at Summit during May–June in 2007 (a), and June–July in 2008 (b) from the SURF (blue lines and boxes) and DEEP (red lines and boxes) simulations, and the long-path differential optical absorption spectroscopy observed BrO concentrations from Stutz et al. (2011). Each panel has the time series of BrO (left) and box and whisker plot (right). The DEEP modeled average BrO concentrations are 1.2 and 0.9 ppt for 2007 and 2008 seasons, respectively, similar to the values reported in Stutz et al. (2011).

mean soluble Br^- is 0.5 ppt for both 2007 and 2008 seasons, which are much closer to values reported in Dibb et al. (2010). The discrepancy between these observations has not been reconciled.

In summary, the agreement between the DEEP simulated and the LP-DOAS observed BrO provides some validation to the large emission flux estimated in DEEP, even though LP-DOAS observed BrO is higher compared to the soluble Br^- observations. However, this large emission flux cannot be sustained by current bromine deposition flux in the model, likely due to a combination of overestimated emission and underestimated deposition. It is possible that snow bromine and/or snow oxidants are getting depleted at some point during the sunlit season, and the model lacks atmospheric bromine sources due to unaccounted anthropogenic sources or uncertainties in long-range transport (Thomas et al., 2012b). Alternatively, there may be an unknown source or mechanism (Grannas et al., 2007) that replenishes bromine in the snow photic zone in inland Greenland. Further investigations on the sources, evolution, and loss of snow bromine throughout the sunlit season are crucial for better constraining the deeper snow processes.

3.3. Model Limitations

We implemented a snowpack bromine emission scheme into a global chemical transport model based on previous 1D and 3D modeling work (Swanson et al., 2022; Thomas et al., 2011; Toyota et al., 2011, 2014). Unlike

previous global models, our model explicitly tracked snow bromide in surface skin layer, shut down bromine emissions when surface melting occurs (Burd et al., 2017; Jeong et al., 2022), and separately represented the deposition-driven bromine recycling at the surface skin layer and the photochemistry-driven deeper snow reactive bromine production.

A major limitation of our global model is that it does not have an explicit representation of physical processes in the snow pack. Production of reactive bromine from deeper in the snow beneath the surface skin layer is calculated in our model using a simplified parameterization based on results from 1D snow-atmosphere models constrained by field observations (Thomas et al., 2011; Toyota et al., 2014). The 1D snow models on which the deeper snow production of reactive bromine was based were run over short time periods (3–8 days) during the spring (Toyota et al., 2014) or summer (Thomas et al., 2011), and compared well with concurrent surface observations (Liao et al., 2011; Stutz et al., 2011). Our simplified parameterization based on these 1D models resulted in an overestimate of reactive bromine emissions from beneath the snow skin layer over an annual cycle. Apart from the underestimation in atmospheric Br_y deposition, this could also suggest that the photochemical reactivity of snow bromide in snow layers below the surface skin layer decreases over time after polar sunrise, and may become the major limiting factor for photochemical reactive bromine production in snowpack later in the sunlit season. A recent laboratory study found a factor of 4–7 decrease in heterogeneous reactivity of bromine in snow after 12 days of temperature gradient dry metamorphism, likely due to the burial of bromide during the process and the subsequent absence of bromide at the air-ice interface (Edebeli et al., 2020). However, DOAS measurements at Summit during May-June, 2007 and June-July, 2008 show no drop in BrO concentrations in late summer (Stutz et al., 2011). The timing and extent of decrease in chemically reactive bromine needs further investigation.

In the model configurations employed in the previous and present studies, the photochemical reactivity of bromide captured by snow grains is pre-determined in ad-hoc manners, both in deeper layers and at the surface. For surface snow, we assume that only dry deposited bromide is photochemically reactive, effectively assuming that wet deposited bromine is encapsulated in snow grains and unavailable for surface reactions (Text S1 in Supporting Information S1). In their 1D snow modeling studies, Thomas et al. (2011) assumed that all bromide measured in surface melted snow is located in the liquid like layer (LLL) on snow grains and is thus photochemically reactive, while Toyota et al. (2014) calculated the reactive concentration of bromine at the surface of the snow grains by scaling the bulk bromine concentrations by the volume fraction of the LLL. Additional lab studies aimed at better understanding the details of the photochemical reactivity of snow bromine and how it evolves over time are required to inform model development efforts and improve our ability to quantify bromine preservation in the snowpack.

In addition, the impact of snow acidity variations on the efficiency of bromine release is not considered in our model and is thus a source of uncertainty. Major bromine heterogeneous reactions occurring in snowpack are acid-catalyzed (R6, R7, and R9), and snow pH was shown to be important for the production of reactive bromine in snow in field experiments (Pratt et al., 2013) and lab studies (Wren et al., 2013). The ice cores presented here are acidic enough (average pH = 5.4, Figure S1 in Supporting Information S1) to facilitate acid-catalyzed heterogeneous reactions (Pratt et al., 2013), but the relationship between the acidity of the bulk and the LLL is unknown. Also unknown is the importance of variations in snow acidity over time, such as varying acidity over the industrial era due to anthropogenic activities or spikes in acidity due to volcanic activity (Figure S1 in Supporting Information S1).

4. Conclusions and Recommendations for Future Work

Snowpack bromine emissions are an important local source of reactive bromine over snow covered regions and are needed to explain spring Arctic ODEs (Swanson et al., 2022; Jeong et al., 2022, etc.). In contrast, loss of bromine from the snow has been considered negligible in the interpretation of long-term ice core bromine trends (Vallelonga et al., 2021). To investigate the impact of snowpack release of bromine on post-depositional loss in ice cores, we analyzed bromine trends from six Arctic ice cores dated since the pre-industrial. Among the six ice cores analyzed, the coastal Arctic ice core, AN, is the only core that shows significant trends in both Br_{exc} and Br_{enr}. The timing and direction of the observed trends in the AN core are consistent with trends in atmospheric acidity and anthropogenic emissions of bromine from leaded gasoline since 1940, and are also consistent with observed trends in sea ice extent since at least 1979.

We implemented snow bromine chemistry into a global three-dimensional model to estimate snow bromine preservation at the six ice core locations using several different assumptions. Model simulations with surface recycling show moderate snow bromine loss that is similar among the six ice core locations (9–17%). Model results with simplified photochemical bromine loss deeper in the snow beneath the skin layer suggest that photochemistry occurring in deeper snow within the snow photic zone may dominate snowpack emissions of bromine, consistent with previous modeling studies at coastal locations (Toyota et al., 2014). However, model estimates of deeper snow production over the course of a full year are unrealistically high relative to surface deposition fluxes. Model simulations that include surface recycling only, with no deeper production, agree with observations of atmospheric soluble bromine in May, June, and July at Summit, Greenland (Dibb et al., 2010), but deeper snow production is needed to explain the observed BrO (Stutz et al., 2011). Quantifying the sources of snow bromine and the extent of bromine loss within the snow photic zone beneath the skin layer is key to understanding the extent of post-depositional loss of bromine in ice cores.

We hypothesize that snow bromine loss peaks in early spring after polar sunrise because snow Br^- concentrations are highest then. As the sunlit portion of the year progresses, the amount of photochemically reactive snow Br^- is depleted and becomes a limiting factor for deeper snow production of reactive bromine. We suggest that some portion of snow bromine is not photochemically reactive and is preserved in the snowpack, and hypothesize that this may be related to the fraction of bromine that is wet deposited to the snowpack (Text S1 in Supporting Information S1). If this is true, ice-core sites with higher amounts of wet deposition will be more likely to preserve atmospheric bromine trends. The availability and reactivity of wet deposited bromine species remain largely unknown and requires detailed observational and lab investigations (Bartels-Rausch et al., 2014).

The potentially significant snow bromine loss calculated in our model suggests that photochemical loss of snow bromine must be considered when interpreting ice core bromine records. Current modeling efforts lack knowledge on the photochemical reactivity of snow bromine in the snow photic zone and how it evolves throughout the sunlit season, especially in inland Arctic sites. Improving our understanding of ice-core bromine preservation requires lab studies investigating the microphysics of snow grain structure, the reactivity of snow bromine as a function of location in the snow grain, and how this might evolve over time through processes such as snow sublimation, metamorphism, melting and refreezing. It is also essential to determine how emissions of reactive bromine from the snow evolve throughout the sunlit portion of the year, particularly for inland locations where ice cores are drilled. This could be accomplished through field studies comparing fluxes and concentrations of atmospheric and snow bromine at different times during the spring and summer.

Despite the model overestimate of loss of bromine from the deeper snow layers, the AN ice core still shows significant preservation of bromine in the model for all sensitivity simulations, consistent with the observation that it is the only ice core that demonstrates significant trends since the pre-industrial. In contrast, the large bromine loss modeled in Greenland supports the lack of trends in Greenland ice core bromine records. The AN core is also the only ice core that has snow layers that are relatively isolated from sunlight due to the high snow accumulation rate and relatively long polar night (Text S1 in Supporting Information S1). The observed trends in AN total bromine are qualitatively consistent with observed trends in a mid-latitude ice core, CDD (Legrand et al., 2021). The trends in the CDD ice core were mainly attributed to trends in emissions of bromine from leaded gasoline, which was phased out in Europe in 1970s (Lammel et al., 2002). This study does not quantify the role of anthropogenic emissions (including acidity and gasoline usage) or sea ice extent in regulating trends observed in the AN core. We will examine this in a follow-up study.

Data Availability Statement

Ice-core data for this research can be downloaded from the Arctic Data Center with Creative Commons Attribution (https://arcticdata.io/catalog/view/doi:10.18739/A2K649V3D). GEOS-Chem is open software and available on https://doi.org/10.5281/zenodo.5047976. GEOS-Chem with snowpack bromine chemistry simulations output is archived in the Dryad Data Repository (https://datadryad.org/stash/dataset/doi:10.5061/dryad.3j9kd51r4).

Acknowledgments
Becky Alexander and Shuting Zhai acknowledge support from U.S. National Science Foundation (NSF) grants AGS 2202287 and 1702266. William Swanson acknowledges NSF grant ARC 1602716. This publication is partially funded by the Cooperative Institute for Climate, Ocean, & Ecosystem Studies (CICOES) under NOAA Cooperative Agreement NA20OAR4320271, Contribution No. 2023-1261. For the ice-core data, Joseph R. McConnell acknowledges support from NSF grants 0909541, 1023672, 1204176, and 1702830. The authors also thank the Danish-led North Greenland Eemian Ice Drilling (NEEM) consortium, the Alfred Wegener Institute, the U.S. Ice Drilling Program, as well as staff and students of the DRI ice-core laboratory including O. Maselli, D.Pasteris, and L. Layman. Jochen Stutz and Jack E. Dibb thank the NSF GEO ATM (now AGS) Tropospheric Chemistry program for funding (GrantATM-0612279:002) of the GSHOx campaign and the NSF OPP Arctic Research Support and Logistics program and CH2M Hill Polar Services for logistic support. Becky Alexander and Shuting Zhai acknowledge fruitful discussions with Jennie L. Thomas. Shuting Zhai appreciates help from Eric Ruggieri on the changepoint analysis.

References

Abbatt, J. P. D., Oldridge, N., Symington, A., Chukalovskiy, V., McWhinney, R. D., Sjostedt, S., & Cox, R. A. (2010). Release of gas-phase halogens by photolytic generation of OH in frozen halide-nitrate solutions: An active halogen formation mechanism? *The Journal of Physical Chemistry A*, *114*(23), 6527–6533. https://doi.org/10.1021/jp102072t

Abbatt, J. P. D., Thomas, J. L., Abrahamsson, K., Boxe, C., Granfors, A., Jones, A. E., et al. (2012). Halogen activation via interactions with environmental ice and snow in the polar lower troposphere and other regions. *Atmospheric Chemistry and Physics*, *12*(14), 6237–6271. https://doi.org/10.5194/acp-12-6237-2012

Ahmed, S., Thomas, J. L., Tuite, K., Stutz, J., Flocke, F., Orlando, J. J., et al. (2022). The role of snow in controlling halogen chemistry and boundary layer oxidation during arctic spring: A 1D modeling case study. *Journal of Geophysical Research: Atmospheres*, *127*(5), e2021JD036140. https://doi.org/10.1029/2021jd036140

Aiuppa, A., Federico, C., Franco, A., Giudice, G., Gurrieri, S., Inguaggiato, S., et al. (2005). Emission of bromine and iodine from Mount Etna volcano. *Geochemistry, Geophysics, Geosystems*, *6*(8). https://doi.org/10.1029/2005gc000965

Amos, H. M., Jacob, D. J., Holmes, C. D., Fisher, J. A., Wang, Q., Yantosca, R. M., et al. (2012). Gas-particle partitioning of atmospheric Hg(II) and its effect on global mercury deposition. *Atmospheric Chemistry and Physics*, *12*(1), 591–603. https://doi.org/10.5194/acp-12-591-2012

Barrie, L. A., Bottenheim, J. W., Schnell, R. C., Crutzen, P. J., & Rasmussen, R. A. (1988). Ozone destruction and photochemical reactions at polar sunrise in the lower Arctic atmosphere. *Nature*, *334*(6178), 138–141. https://doi.org/10.1038/334138a0

Bartels-Rausch, T., Jacobi, H.-W., Kahan, T. F., Thomas, J. L., Thomson, E. S., Abbatt, J. P. D., et al. (2014). A review of air–ice chemical and physical interactions (AICI): Liquids, quasi-liquids, and solids in snow. *Atmospheric Chemistry and Physics*, *14*(3), 1587–1633. https://doi.org/10.5194/acp-14-1587-2014

Benavent, N., Mahajan, A. S., Li, Q., Cuevas, C. A., Schmale, J., Angot, H., et al. (2022). Substantial contribution of iodine to Arctic ozone destruction. *Nature Geoscience*, *15*(10), 770–773. https://doi.org/10.1038/s41561-022-01018-w

Bobrowski, N., Hönninger, G., Galle, B., & Platt, U. (2003). Detection of bromine monoxide in a volcanic plume. *Nature*, *423*(6937), 273–276. https://doi.org/10.1038/nature01625

Bougoudis, I., Blechschmidt, A.-M., Richter, A., Seo, S., Burrows, J. P., Theys, N., & Rinke, A. (2020). Long-term time series of Arctic tropospheric BrO derived from UV–VIS satellite remote sensing and its relation to first-year sea ice. *Atmospheric Chemistry and Physics*, *20*(20), 11869–11892. https://doi.org/10.5194/acp-20-11869-2020

Bourgeois, C. S., Calanca, P., & Ohmura, A. (2006). A field study of the hemispherical directional reflectance factor and spectral albedo of dry snow. *Journal of Geophysical Research*, *111*(D20), D20108. https://doi.org/10.1029/2006jd007296

Brennan, K. M., & Hakim, G. J. (2021). Reconstructing Arctic sea ice over the common era using data assimilation. *Journal of Climate*, *1*(aop), 1–55. https://doi.org/10.1175/JCLI-D-21-0099.1

Burd, J. A., Peterson, P. K., Nghiem, S. V., Perovich, D. K., & Simpson, W. R. (2017). Snowmelt onset hinders bromine monoxide heterogeneous recycling in the Arctic. *Journal of Geophysical Research: Atmospheres*, *122*(15), 8297–8309. https://doi.org/10.1002/2017JD026906

Chen, Q., Schmidt, J. A., Shah, V., Jaeglé, L., Sherwen, T., & Alexander, B. (2017). Sulfate production by reactive bromine: Implications for the global sulfur and reactive bromine budgets: Sulfur-Halogen Interactions. *Geophysical Research Letters*, *44*(13), 7069–7078. https://doi.org/10.1002/2017GL073812

Clerbaux, C., Cunnold, D. M., Anderson, J., Engel, A., Fraser, P. J., Mahieu, E., et al. (2007). *Scientific assessment of ozone depletion: 2006*. Global Ozone Research and Monitoring Project - Report No. 50. Retrieved from https://agris.fao.org/agris-search/search.do?recordID=BE2014102317

Cole-Dai, J., Ferris, D. G., Lanciki, A. L., Savarino, J., Thiemens, M. H., & McConnell, J. R. (2013). Two likely stratospheric volcanic eruptions in the 1450s C.E. found in a bipolar, subannually dated 800 year ice core record: Two volcanic eruptions in the 1450s. *Journal of Geophysical Research: Atmospheres*, *118*(14), 7459–7466. https://doi.org/10.1002/jgrd.50587

Comiso, J. C., Meier, W. N., & Gersten, R. (2017). Variability and trends in the Arctic Sea ice cover: Results from different techniques. *Journal of Geophysical Research: Oceans*, *122*(8), 6883–6900. https://doi.org/10.1002/2017jc012768

Custard, K. D., Pratt, K. A., Wang, S., & Shepson, P. B. (2016). Constraints on Arctic Atmospheric chlorine production through measurements and simulations of Cl2 and ClO. *Environmental Science & Technology*, *50*(22), 12394–12400. https://doi.org/10.1021/acs.est.6b03909

Custard, K. D., Raso, A. R. W., Shepson, P. B., Staebler, R. M., & Pratt, K. A. (2017). Production and release of molecular bromine and chlorine from the Arctic coastal snowpack. *ACS Earth and Space Chemistry*, *1*(3), 142–151. https://doi.org/10.1021/acsearthspacechem.7b00014

Dibb, J. E., Ziemba, L. D., Luxford, J., & Beckman, P. (2010). Bromide and other ions in the snow, firn air, and atmospheric boundary layer at Summit during GSHOX. *Atmospheric Chemistry and Physics*, *10*(20), 9931–9942. https://doi.org/10.5194/acp-10-9931-2010

Domine, F., Bock, J., Voisin, D., & Donaldson, D. J. (2013). Can we model snow photochemistry? Problems with the current approaches. *The Journal of Physical Chemistry A*, *117*(23), 4733–4749. https://doi.org/10.1021/jp3123314

Domine, F., Sparapani, R., Ianniello, A., & Beine, H. J. (2004). The origin of sea salt in snow on Arctic sea ice and in coastal regions. *Atmospheric Chemistry and Physics*, *4*(9/10), 2259–2271. https://doi.org/10.5194/acp-4-2259-2004

Eastham, S. D., Weisenstein, D. K., & Barrett, S. R. H. (2014). Development and evaluation of the unified tropospheric–stratospheric chemistry extension (UCX) for the global chemistry-transport model GEOS-Chem. *Atmospheric Environment*, *89*, 52–63. https://doi.org/10.1016/j.atmosenv.2014.02.001

Edebeli, J., Trachsel, J. C., Avak, S. E., Ammann, M., Schneebeli, M., Eichler, A., & Bartels-Rausch, T. (2020). Snow heterogeneous reactivity of bromide with ozone lost during snow metamorphism. *Atmospheric Chemistry and Physics*, *20*(21), 13443–13454. https://doi.org/10.5194/acp-20-13443-2020

Erbland, J., Vicars, W. C., Savarino, J., Morin, S., Frey, M. M., Frosini, D., et al. (2013). Air–snow transfer of nitrate on the East Antarctic Plateau – Part 1: Isotopic evidence for a photolytically driven dynamic equilibrium in summer. *Atmospheric Chemistry and Physics*, *13*(13), 6403–6419. https://doi.org/10.5194/acp-13-6403-2013

Falk, S., & Sinnhuber, B.-M. (2018). Polar boundary layer bromine explosion and ozone depletion events in the chemistry–climate model EMAC v2.52: Implementation and evaluation of AirSnow algorithm [Dataset]. Geoscientific Model Development, *11*(3), 1115–1131. https://doi.org/10.5194/gmd-11-1115-2018

Foster, K. L., Plastridge, R. A., Bottenheim, J. W., Shepson, P. B., Finlayson-Pitts, B. J., & Spicer, C. W. (2001). The role of Br2 and BrCl in surface ozone destruction at polar sunrise. *Science*, *291*(5503), 471–474. https://doi.org/10.1126/science.291.5503.471

Fritzsche, D., Wilhelms, F., Savatyugin, L. M., Pinglot, J. F., Meyer, H., Hubberten, H.-W., & Miller, H. (2002). A new deep ice core from Akademii Nauk ice cap, Severnaya Zemlya, Eurasian Arctic: First results. *Annals of Glaciology*, *35*, 25–28. https://doi.org/10.3189/172756402781816645

Gelaro, R., McCarty, W., Suárez, M. J., Todling, R., Molod, A., Takacs, L., et al. (2017). The modern-era retrospective analysis for research and applications, version 2 (MERRA-2). *Journal of Climate*, *30*(13), 5419–5454. https://doi.org/10.1175/JCLI-D-16-0758.1

Ghosal, S., Hemminger, J. C., Bluhm, H., Mun, B. S., Hebenstreit, E. L. D., Ketteler, G., et al. (2005). Electron spectroscopy of aqueous solution interfaces reveals surface enhancement of halides. *Science*, *307*(5709), 563–566. https://doi.org/10.1126/science.1106525

Ghosal, S., Shbeeb, A., & Hemminger, J. C. (2000). Surface segregation of bromine in bromide doped NaCl: Implications for the seasonal variations in Arctic ozone. *Geophysical Research Letters*, *27*(13), 1879–1882. https://doi.org/10.1029/2000gl011381

Gladich, I., Shepson, P. B., Carignano, M. A., & Szleifer, I. (2011). Halide affinity for the water-air interface in aqueous solutions of mixtures of sodium salts. *The Journal of Physical Chemistry A*, *115*(23), 5895–5899. https://doi.org/10.1021/jp110208a

Grannas, A. M., Jones, A. E., Dibb, J., Ammann, M., Anastasio, C., Beine, H. J., et al. (2007). An overview of snow photochemistry: Evidence, mechanisms and impacts. *Atmospheric Chemistry and Physics*, *7*(16), 4329–4373. https://doi.org/10.5194/acp-7-4329-2007

Habibi, K. (1973). Characterization of particulate matter in vehicle exhaust. *Environmental Science & Technology*, *7*(3), 223–234. https://doi.org/10.1021/es60075a001

Hara, K., Osada, K., Matsunaga, K., Iwasaka, Y., Shibata, T., & Furuya, K. (2002). Atmospheric inorganic chlorine and bromine species in Arctic boundary layer of the winter/spring. *Journal of Geophysical Research*, *107*(D18), AAC-4.

Hebestreit, K., Stutz, J., Rosen, D., Matveiv, V., Peleg, M., Luria, M., & Platt, U. (1999). DOAS measurements of tropospheric bromine oxide in mid-latitudes. *Science*, *283*(5398), 55–57. https://doi.org/10.1126/science.283.5398.55

Herrmann, M., Schöne, M., Borger, C., Warnach, S., Wagner, T., Platt, U., & Gutheil, E. (2022). Ozone depletion events in the Arctic spring of 2019: A new modeling approach to bromine emissions. *Atmospheric Chemistry and Physics*, *22*(20), 13495–13526. https://doi.org/10.5194/acp-22-13495-2022

Herrmann, M., Sihler, H., Frieß, U., Wagner, T., Platt, U., & Gutheil, E. (2021). Time-dependent 3D simulations of tropospheric ozone depletion events in the Arctic spring using the Weather Research and Forecasting model coupled with Chemistry (WRF-Chem). *Atmospheric and Climate Sciences*, *21*(10), 7611–7638. https://doi.org/10.5194/acp-21-7611-2021

Horowitz, H. M., Jacob, D. J., Zhang, Y., Dibble, T. S., Slemr, F., Amos, H. M., et al. (2017). A new mechanism for atmospheric mercury redox chemistry: Implications for the global mercury budget. *Atmospheric Chemistry and Physics*, *17*(10), 6353–6371. https://doi.org/10.5194/acp-17-6353-2017

Huang, J., & Jaeglé, L. (2017). Wintertime enhancements of sea salt aerosol in polar regions consistent with a sea ice source from blowing snow. *Atmospheric Chemistry and Physics*, *17*(5), 3699–3712. https://doi.org/10.5194/acp-17-3699-2017

Huang, J., Jaeglé, L., Chen, Q., Alexander, B., Sherwen, T., Evans, M. J., et al. (2020). Evaluating the impact of blowing-snow sea salt aerosol on springtime BrO and O 3 in the Arctic. *Atmospheric Chemistry and Physics*, *20*(12), 7335–7358. https://doi.org/10.5194/acp-20-7335-2020

Jeong, D., McNamara, S. M., Barget, A. J., Raso, A. R. W., Upchurch, L. M., Thanekar, S., et al. (2022). Multiphase reactive bromine chemistry during late spring in the Arctic: Measurements of gases, particles, and snow. *ACS Earth and Space Chemistry*, *6*(12), 2877–2887. https://doi.org/10.1021/acsearthspacechem.2c00189

Kerkweg, A., Jöckel, P., Pozzer, A., Tost, H., Sander, R., Schulz, M., et al. (2008). Consistent simulation of bromine chemistry from the marine boundary layer to the stratosphere – Part 1: Model description, sea salt aerosols and pH. *Atmospheric Chemistry and Physics*, *8*(19), 5899–5917. https://doi.org/10.5194/acp-8-5899-2008

Koop, T., Kapilashrami, A., Molina, L. T., & Molina, M. J. (2000). Phase transitions of sea-salt/water mixtures at low temperatures: Implications for ozone chemistry in the polar marine boundary layer. *Journal of Geophysical Research*, *105*(D21), 26393–26402. https://doi.org/10.1029/2000jd900413

Lammel, G., Röhrl, A., & Schreiber, H. (2002). Atmospheric lead and bromine in Germany. *Environmental Science and Pollution Research*, *9*(6), 397–404. https://doi.org/10.1007/BF02987589

Lee, B. H., Lopez-Hilfiker, F. D., Schroder, J. C., Campuzano-Jost, P., Jimenez, J. L., McDuffie, E. E., et al. (2018). Airborne observations of reactive inorganic chlorine and bromine species in the exhaust of coal-fired power plants. *Journal of Geophysical Research: Atmospheres*, *123*(19), 11225–11237. https://doi.org/10.1029/2018JD029284

Lee-Taylor, J., & Madronich, S. (2002). Calculation of actinic fluxes with a coupled atmosphere–snow radiative transfer model. *Journal of Geophysical Research*, *107*(D24), ACH22-1–ACH22-10. https://doi.org/10.1029/2002jd002084

Legrand, M., McConnell, J. R., Preunkert, S., Chellman, N. J., & Arienzo, M. (2021). Causes of enhanced bromine levels in Alpine ice cores during the 20th century: Implications for bromine in the free European troposphere. *Journal of Geophysical Research: Atmospheres*, *126*(8), e2020JD034246. https://doi.org/10.1029/2020jd034246

Lehrer, E., Hönninger, G., & Platt, U. (2004). A one dimensional model study of the mechanism of halogen liberation and vertical transport in the polar troposphere. *Atmospheric Chemistry and Physics*, *4*(11/12), 2427–2440. https://doi.org/10.5194/acp-4-2427-2004

Liang, Q., Atlas, E., Blake, D., Dorf, M., Pfeilsticker, K., & Schauffler, S. (2014). Convective transport of very short lived bromocarbons to the stratosphere. *Atmospheric Chemistry and Physics*, *14*(11), 5781–5792. https://doi.org/10.5194/acp-14-5781-2014

Liang, Q., Stolarski, R. S., Kawa, S. R., Nielsen, J. E., Douglass, A. R., Rodriguez, J. M., et al. (2010). Finding the missing stratospheric Br_y: A global modeling study of $CHBr_3$ and CH_2Br_2. *Atmospheric Chemistry and Physics*, *10*(5), 2269–2286. https://doi.org/10.5194/acp-10-2269-2010

Liao, J., Huey, L. G., Liu, Z., Tanner, D. J., Cantrell, C. A., Orlando, J. J., et al. (2014). High levels of molecular chlorine in the Arctic atmosphere. *Nature Geoscience*, *7*(2), 91–94. https://doi.org/10.1038/ngeo2046

Liao, J., Huey, L. G., Scheuer, E., Dibb, J. E., Stickel, R. E., Tanner, D. J., et al. (2011a). Characterization of soluble bromide measurements and a case study of BrO observations during ARCTAS. *Atmospheric Chemistry and Physics Discussions*, *11*(9), 8577–8591. https://doi.org/10.5194/acp-11-8577-2011

Liao, J., Huey, L. G., Tanner, D. J., Brough, N., Brooks, S., Dibb, J. E., et al. (2011). Observations of hydroxyl and peroxy radicals and the impact of BrO at Summit, Greenland in 2007 and 2008. *Atmospheric Chemistry and Physics*, *11*(16), 8577–8591. https://doi.org/10.5194/acp-11-8577-2011

Liao, J., Huey, L. G., Tanner, D. J., Flocke, F. M., Orlando, J. J., Neuman, J. A., et al. (2012). Observations of inorganic bromine (HOBr, BrO, and Br2) speciation at Barrow, Alaska, in spring 2009. *Journal of Geophysical Research*, *117*(D14). https://doi.org/10.1029/2011jd016641

Liao, J., Sihler, H., Huey, L. G., Neuman, J. A., Tanner, D. J., Friess, U., et al. (2011). A comparison of Arctic BrO measurements by chemical ionization mass spectrometry and long path-differential optical absorption spectroscopy. *Journal of Geophysical Research*, *116*(D00R02), D00R02. https://doi.org/10.1029/2010jd014788

Liu, H., Jacob, D. J., Bey, I., & Yantosca, R. M. (2001). Constraints from210Pb and7Be on wet deposition and transport in a global three-dimensional chemical tracer model driven by assimilated meteorological fields. *Journal of Geophysical Research*, *106*(D11), 12109–12128. https://doi.org/10.1029/2000jd900839

Maffezzoli, N., Risebrobakken, B., Miles, M. W., Vallelonga, P., Berben, S. M. P., Scoto, F., et al. (2021). Sea ice in the northern North Atlantic through the Holocene: Evidence from ice cores and marine sediment records. *Quaternary Science Reviews*, *273*, 107249. https://doi.org/10.1016/j.quascirev.2021.107249

Mahoney, A. R., Barry, R. G., Smolyanitsky, V., & Fetterer, F. (2008). Observed sea ice extent in the Russian Arctic, 1933–2006. *Journal of Geophysical Research*, *113*(C11). https://doi.org/10.1029/2008jc004830

Marelle, L., Thomas, J. L., Ahmed, S., Tuite, K., Stutz, J., Dommergue, A., et al. (2021). Implementation and impacts of surface and blowing snow sources of Arctic bromine activation within WRF-Chem 4.1.1. *Journal of Advances in Modeling Earth Systems*, *13*(8). https://doi.org/10.1029/2020ms002391

Maselli, O. J., Chellman, N. J., Grieman, M., Layman, L., McConnell, J. R., Pasteris, D., et al. (2017). Sea ice and pollution-modulated changes in Greenland ice core methanesulfonate and bromine. *Climate of the Past*, *13*(1), 39–59. https://doi.org/10.5194/cp-13-39-2017

Matveev, V., Peleg, M., Rosen, D., Tov-Alper, D. S., Hebestreit, K., Stutz, J., et al. (2001). Bromine oxide-ozone interaction over the dead sea. *Journal of Geophysical Research*, *106*(D10), 10375–10387. https://doi.org/10.1029/2000jd900611

McConnell, J. R., Burke, A., Dunbar, N. W., Köhler, P., Thomas, J. L., Arienzo, M. M., et al. (2017). Synchronous volcanic eruptions and abrupt climate change∼ 17.7 ka plausibly linked by stratospheric ozone depletion. In *Proceedings of the Estonian Academy of Sciences. Biology, Ecology = Eesti Teaduste Akadeemia Toimetised*. Bioloogia, Okoloogia. Retrieved from https://www.pnas.org/content/114/38/10035?tab=-metrics&utm_source=TrendMD&utm_medium=cpc&utm_campaign=Proc_Natl_Acad_Sci_U_S_A_TrendMD_1

McConnell, J. R., Chellman, N. J., Wilson, A. I., Stohl, A., Arienzo, M. M., Eckhardt, S., et al. (2019). Pervasive Arctic lead pollution suggests substantial growth in medieval silver production modulated by plague, climate, and conflict. *Proceedings of the National Academy of Sciences of the United States of America*, *116*(30), 14910–14915. https://doi.org/10.1073/pnas.1904515116

Michalowski, B. A., Francisco, J. S., Li, S.-M., Barrie, L. A., Bottenheim, J. W., & Shepson, P. B. (2000). A computer model study of multiphase chemistry in the Arctic boundary layer during polar sunrise. *Journal of Geophysical Research*, *105*(D12), 15131–15145. https://doi.org/10.1029/2000jd900004

Millero, F. J., Feistel, R., Wright, D. G., & McDougall, T. J. (2008). The composition of standard seawater and the definition of the reference-composition salinity scale. *Deep Sea Research Part I: Oceanographic Research Papers*, *55*(1), 50–72. https://doi.org/10.1016/j.dsr.2007.10.001

Mozurkewich, M. (1995). Mechanisms for the release of halogens from sea-salt particles by free radical reactions. *Journal of Geophysical Research*, *100*(D7), 14199–14207. https://doi.org/10.1029/94jd00358

Nandan, V., Geldsetzer, T., Yackel, J., Mahmud, M., Scharien, R., Howell, S., et al. (2017). Effect of snow salinity on CryoSat-2 arctic first-year sea ice freeboard measurements. *Geophysical Research Letters*, *44*(20), 10419–10426. https://doi.org/10.1002/2017gl074506

Oltmans, S. J., Johnson, B. J., & Harris, J. M. (2012). Springtime boundary layer ozone depletion at Barrow, Alaska: Meteorological influence, year-to-year variation, and long-term change. *Journal of Geophysical Research*, *117*(D14). https://doi.org/10.1029/2011jd016889

Oltmans, S. J., Schnell, R. C., Sheridan, P. J., Peterson, R. E., Li, S.-M., Winchester, J. W., et al. (1989). Seasonal surface ozone and filterable bromine relationship in the high Arctic. *Atmospheric Environment*, *23*(11), 2431–2441. https://doi.org/10.1016/0004-6981(89)90254-0

Opel, T., Fritzsche, D., & Meyer, H. (2013). Eurasian Arctic climate over the past millennium as recorded in the Akademii Nauk ice core (Severnaya Zemlya). *Climate of the Past*, *9*(5), 2379–2389. https://doi.org/10.5194/cp-9-2379-2013

Oum, K. W., Lakin, M. J., & Finlayson-Pitts, B. J. (1998). Bromine activation in the troposphere by the dark reaction of O3with seawater ice. *Geophysical Research Letters*, *25*(21), 3923–3926. https://doi.org/10.1029/1998gl900078

Pasteris, D. R., McConnell, J. R., & Edwards, R. (2012). High-resolution, continuous method for measurement of acidity in ice cores. *Environmental Science & Technology*, *46*(3), 1659–1666. https://doi.org/10.1021/es202668n

Peterson, P. K., Pöhler, D., Zielcke, J., General, S., Frieß, U., Platt, U., et al. (2018). Springtime bromine activation over coastal and inland Arctic snowpacks. *ACS Earth and Space Chemistry*, *2*(10), 1075–1086. https://doi.org/10.1021/acsearthspacechem.8b00083

Piot, M., & von Glasow, R. (2009). Modelling the multiphase near-surface chemistry related to ozone depletions in polar spring. *Journal of Atmospheric Chemistry*, *64*(2), 77–105. https://doi.org/10.1007/s10874-010-9170-1

Piot, M., & von Glasow, R. (2008). The potential importance of frost flowers, recycling on snow, and open leads for ozone depletion events. *Atmospheric Chemistry and Physics*, *8*(9), 2437–2467. https://doi.org/10.5194/acp-8-2437-2008

Pratt, K. A., Custard, K. D., Shepson, P. B., Douglas, T. A., Pöhler, D., General, S., et al. (2013). Photochemical production of molecular bromine in Arctic surface snowpacks. *Nature Geoscience*, *6*(5), 351–356. https://doi.org/10.1038/ngeo1779

Quack, B., & Wallace, D. W. R. (2003). Air-sea flux of bromoform: Controls, rates, and implications. *Global Biogeochemical Cycles*, *17*(1). https://doi.org/10.1029/2002gb001890

Reeves, C. E. (2003). Atmospheric budget implications of the temporal and spatial trends in methyl bromide concentration. *Journal of Geophysical Research*, *108*(D11), 4343. https://doi.org/10.1029/2002jd002943

Ruggieri, E. (2013). A Bayesian approach to detecting change points in climatic records. *International Journal of Climatology*, *33*(2), 520–528. https://doi.org/10.1002/joc.3447

Sherwen, T., Schmidt, J. A., Evans, M. J., Carpenter, L. J., Großmann, K., Eastham, S. D., et al. (2016). Global impacts of tropospheric halogens (Cl, Br, I) on oxidants and composition in GEOS-Chem. *Atmospheric Chemistry and Physics*, *16*(18), 12239–12271. https://doi.org/10.5194/acp-16-12239-2016

Sigl, M., McConnell, J. R., Layman, L., Maselli, O., McGwire, K., Pasteris, D., et al. (2013). A new bipolar ice core record of volcanism from WAIS Divide and NEEM and implications for climate forcing of the last 2000 years. *Journal of Geophysical Research: Atmospheres*, *118*(3), 1151–1169. https://doi.org/10.1029/2012jd018603

Simpson, W. R., Carlson, D., Hönninger, G., Douglas, T. A., Sturm, M., Perovich, D., & Platt, U. (2007a). First-year sea-ice contact predicts bromine monoxide (BrO) levels at Barrow, Alaska better than potential frost flower contact. *Atmospheric Chemistry and Physics*, *7*(3), 621–627. https://doi.org/10.5194/acp-7-621-2007a

Simpson, W. R., King, M. D., Beine, H. J., Honrath, R. E., & Zhou, X. (2002). Radiation-transfer modeling of snow-pack photochemical processes during ALERT 2000. *Atmospheric Environment*, *36*(15), 2663–2670. https://doi.org/10.1016/S1352-2310(02)00124-3

Simpson, W. R., von Glasow, R., Riedel, K., Anderson, P., Ariya, P., Bottenheim, J., et al. (2007b). Halogens and their role in polar boundary-layer ozone depletion. *Atmospheric Chemistry and Physics Discussions: ACPD*, *7*(2), 4285–4403. https://doi.org/10.5194/acpd-7-4285-2007b

Sjostedt, S. J., & Abbatt, J. P. D. (2008). Release of gas-phase halogens from sodium halide substrates: Heterogeneous oxidation of frozen solutions and desiccated salts by hydroxyl radicals. *Environmental Research Letters: ERL [Web Site]*, *3*(4), 045007. https://doi.org/10.1088/1748-9326/3/4/045007

Spicer, C. W., Plastridge, R. A., Foster, K. L., Finlayson-Pitts, B. J., Bottenheim, J. W., Grannas, A. M., & Shepson, P. B. (2002). Molecular halogens before and during ozone depletion events in the arctic at polar sunrise: Concentrations and sources. *Atmospheric Environment*, *36*(15), 2721–2731. https://doi.org/10.1016/S1352-2310(02)00125-5

Spolaor, A., Gabrieli, J., Martma, T., Kohler, J., Björkman, M. B., Isaksson, E., et al. (2013b). Sea ice dynamics influence halogen deposition to Svalbard. *The Cryosphere*, *7*(5), 1645–1658. https://doi.org/10.5194/tc-7-1645-2013

Spolaor, A., Opel, T., McConnell, J. R., Maselli, O. J., Spreen, G., Varin, C., et al. (2016b). Halogen-based reconstruction of Russian Arctic sea ice area from the Akademii Nauk ice core (Severnaya Zemlya). *The Cryosphere*, *10*(1), 245–256. https://doi.org/10.5194/tc-10-245-2016

Spolaor, A., Vallelonga, P., Plane, J. M. C., Kehrwald, N., Gabrieli, J., Varin, C., et al. (2013a). Halogen species record Antarctic sea ice extent over glacial–interglacial periods. *Atmospheric Chemistry and Physics*, *13*(13), 6623–6635. https://doi.org/10.5194/acp-13-6623-2013

Spolaor, A., Vallelonga, P., Turetta, C., Maffezzoli, N., Cozzi, G., Gabrieli, J., et al. (2016a). Canadian Arctic sea ice reconstructed from bromine in the Greenland NEEM ice core. *Scientific Reports*, *6*(1), 33925. https://doi.org/10.1038/srep33925

Steffen, A., Douglas, T., Amyot, M., Ariya, P., Aspmo, K., Berg, T., et al. (2008). A synthesis of atmospheric mercury depletion event chemistry in the atmosphere and snow. *Atmospheric*, *8*(6), 1445–1482. https://doi.org/10.5194/acp-8-1445-2008

Stutz, J., Thomas, J. L., Hurlock, S. C., Schneider, M., von Glasow, R., Piot, M., et al. (2011). Longpath DOAS observations of surface BrO at Summit, Greenland. *Atmospheric Chemistry and Physics*, *11*(18), 9899–9910. https://doi.org/10.5194/acp-11-9899-2011

Swanson, W. F., Holmes, C. D., Simpson, W. R., Confer, K., Marelle, L., Thomas, J. L., et al. (2022). Comparison of model and ground observations finds snowpack and blowing snow aerosols both contribute to Arctic tropospheric reactive bromine. *Atmospheric Chemistry and Physics*, *22*(22), 14467–14488. https://doi.org/10.5194/acp-22-14467-2022

Thomas, J. L., Dibb, J. E., Huey, L. G., Liao, J., Tanner, D., Lefer, B., et al. (2012a). Modeling chemistry in and above snow at Summit, Greenland – Part 2: Impact of snowpack chemistry on the oxidation capacity of the boundary layer. *Atmospheric Chemistry and Physics*, *12*(14), 6537–6554. https://doi.org/10.5194/acp-12-6537-2012

Thomas, J. L., Dibb, J. E., Stutz, J., von Glasow, R., Brooks, S., Huey, L. G., & Lefer, B. (2012b). Overview of the 2007 and 2008 campaigns conducted as part of the Greenland Summit Halogen-HOx experiment (GSHOX). *Atmospheric Chemistry and Physics*, *12*(22), 10833–10839. https://doi.org/10.5194/acp-12-10833-2012

Thomas, J. L., Stutz, J., Lefer, B., Huey, L. G., Toyota, K., Dibb, J. E., & von Glasow, R. (2011). Modeling chemistry in and above snow at Summit, Greenland – Part 1: Model description and results. *Atmospheric Chemistry and Physics*, *11*(10), 4899–4914. https://doi.org/10.5194/acp-11-4899-2011

Thomas, V. M., Bedford, J. A., & Cicerone, R. J. (1997). Bromine emissions from leaded gasoline. *Geophysical Research Letters*, *24*(11), 1371–1374. https://doi.org/10.1029/97gl01243

Toyota, K., McConnell, J. C., Lupu, A., Neary, L., McLinden, C. A., Richter, A., et al. (2011). Analysis of reactive bromine production and ozone depletion in the arctic boundary layer using 3-D simulations with GEM-AQ: Inference from synoptic-scale patterns. *Atmospheric Chemistry and Physics*, *11*(8), 3949–3979. https://doi.org/10.5194/acp-11-3949-2011

Toyota, K., McConnell, J. C., Staebler, R. M., & Dastoor, A. P. (2014). Air--snowpack exchange of bromine, ozone and mercury in the springtime Arctic simulated by the 1-D model PHANTAS--Part 1: In-snow bromine activation and its impact on ozone. *Atmospheric Chemistry and Physics*, *14*(8), 4101–4133. https://doi.org/10.5194/acp-14-4101-2014

Vallelonga, P., Maffezzoli, N., Saiz-Lopez, A., Scoto, F., Kjær, H. A., & Spolaor, A. (2021). Sea-ice reconstructions from bromine and iodine in ice cores. *Quaternary Science Reviews*, *269*, 107133. https://doi.org/10.1016/j.quascirev.2021.107133

von Glasow, R., von Kuhlmann, R., Lawrence, M. G., Platt, U., & Crutzen, P. J. (2004). Impact of reactive bromine chemistry in the troposphere. *Atmospheric Chemistry and Physics*, *4*(11/12), 2481–2497. https://doi.org/10.5194/acp-4-2481-2004

Wang, S., & Pratt, K. A. (2017). Molecular halogens above the arctic snowpack: Emissions, diurnal variations, and recycling mechanisms. *Journal of Geophysical Research: Atmospheres*, *122*(21), 11991–12007. https://doi.org/10.1002/2017jd027175

Wang, X., Jacob, D. J., Downs, W., Zhai, S., Zhu, L., Shah, V., et al. (2021). Global tropospheric halogen (Cl, Br, I) chemistry and its impact on oxidants. *Atmospheric Chemistry and Physics*. https://doi.org/10.5194/acp-2021-441

Wang, X., Jacob, D. J., Eastham, S. D., Sulprizio, M. P., Zhu, L., Chen, Q., et al. (2019). The role of chlorine in global tropospheric chemistry. *Atmospheric Chemistry and Physics*, *19*(6), 3981–4003. https://doi.org/10.5194/acp-19-3981-2019

Wang, Y., Jacob, D. J., & Logan, J. A. (1998). Global simulation of tropospheric O3-NO x-hydrocarbon chemistry: 1. Model formulation. *Journal of Geophysical Research*, *103*(D9), 10713–10725. https://doi.org/10.1029/98jd00158

Warren, S. G. (1982). Optical properties of snow. *Reviews of Geophysics*, *20*(1), 67–89. https://doi.org/10.1029/RG020i001p00067

Wesely, M. L. (1989). Parameterization of surface resistances to gaseous dry deposition in regional-scale numerical models. *Atmospheric Environment*, *23*(6), 1293–1304. https://doi.org/10.1016/0004-6981(89)90153-4

Wren, S. N., Donaldson, D. J., & Abbatt, J. P. D. (2013). Photochemical chlorine and bromine activation from artificial saline snow. *Atmospheric Chemistry and Physics*, *13*(19), 9789–9800. https://doi.org/10.5194/acp-13-9789-2013

Wren, S. N., Kahan, T. F., Jumaa, K. B., & Donaldson, D. J. (2010). Spectroscopic studies of the heterogeneous reaction between O 3 (g) and halides at the surface of frozen salt solutions. *Journal of Geophysical Research*, *115*(D16), 660. https://doi.org/10.1029/2010JD013929

Yang, X., Cox, R. A., Warwick, N. J., Pyle, J. A., Carver, G. D., O'Connor, F. M., & Savage, N. H. (2005). Tropospheric bromine chemistry and its impacts on ozone: A model study. *Journal of Geophysical Research*, *110*(D23), 3719. https://doi.org/10.1029/2005JD006244

Yang, X., Pyle, J. A., & Cox, R. A. (2008). Sea salt aerosol production and bromine release: Role of snow on sea ice. *Geophysical Research Letters*, *35*(16), L16815. https://doi.org/10.1029/2008gl034536

Zhai, S., Wang, X., McConnell, J. R., Geng, L., Cole-Dai, J., Sigl, M., et al. (2021). Anthropogenic impacts on tropospheric reactive chlorine since the preindustrial. *Geophysical Research Letters*, *48*(14), e2021GL093808. https://doi.org/10.1029/2021gl093808

References From the Supporting Information

Akers, P. D., Savarino, J., Caillon, N., Magand, O., & Le Meur, E. (2022). Photolytic modification of seasonal nitrate isotope cycles in East Antarctica. *EGUsphere*. https://doi.org/10.5194/egusphere-2022-812

Beine, H., Anastasio, C., Esposito, G., Patten, K., Wilkening, E., Domine, F., et al. (2011). Soluble, light-absorbing species in snow at Barrow, Alaska. *Journal of Geophysical Research*, *116*(D00R05), D00R05. https://doi.org/10.1029/2011jd016181

Colosio, P., Tedesco, M., Ranzi, R., & Fettweis, X. (2021). Surface melting over the Greenland ice sheet derived from enhanced resolution passive microwave brightness temperatures (1979–2019). *The Cryosphere*, *15*(6), 2623–2646. https://doi.org/10.5194/tc-15-2623-2021

Galbavy, E. S., Anastasio, C., Lefer, B., & Hall, S. (2007). Light penetration in the snowpack at Summit, Greenland: Part 2 nitrate photolysis. *Atmospheric Environment*, *41*(24), 5091–5100. https://doi.org/10.1016/j.atmosenv.2006.01.066

Kim, Y., Kimball, J. S., Du, J., Schaaf, C. L. B., & Kirchner, P. B. (2018). Quantifying the effects of freeze-thaw transitions and snowpack melt on land surface albedo and energy exchange over Alaska and Western Canada. *Environmental Research Letters: ERL [Web Site]*, *13*(7), 075009. https://doi.org/10.1088/1748-9326/aacf72

Parizek, B. R., & Alley, R. B. (2004). Implications of increased Greenland surface melt under global-warming scenarios: Ice-sheet simulations. *Quaternary Science Reviews*, *23*(9), 1013–1027. https://doi.org/10.1016/j.quascirev.2003.12.024

Winton, V. H. L., Ming, A., Caillon, N., Hauge, L., Jones, A. E., Savarino, J., et al. (2020). Deposition, recycling, and archival of nitrate stable isotopes between the air–snow interface: Comparison between dronning Maud land and Dome C, Antarctica. *Atmospheric Chemistry and Physics*, *20*(9), 5861–5885. https://doi.org/10.5194/acp-20-5861-2020

Journal of Geophysical Research: Atmospheres

Supporting Information for

Implications of Snowpack Reactive Bromine Production for Arctic Ice Core Bromine Preservation

Shuting Zhai[1], William Swanson[2], Joseph R. McConnell[3], Nathan Chellman[3], Thomas Opel[4], Michael Sigl[5], Hanno Meyer[4], Xuan Wang[6,7], Lyatt Jaeglé[1], Jochen Stutz[8], Jack E. Dibb[9], Koji Fujita[10], Becky Alexander[1]

[1]Department of Atmospheric Sciences, University of Washington, Seattle, Washington, US.

[2]Department of Chemistry and Biochemistry and Geophysical Institute, University of Alaska Fairbanks, Fairbanks, Alaska, US.

[3]Division of Hydrologic Sciences, Desert Research Institute, Reno, NV, US.

[4]Alfred-Wegener Institut, Potsdam, Germany.

[5]Climate and Environmental Physics, University of Bern, Bern, Switzerland.

[6]School of Energy and Environment, City University of Hong Kong, Hong Kong SAR, China.

[7]City University of Hong Kong Shenzhen Research Institute, Shenzhen, China.

[8]University of California, Los Angeles; Department of Atmospheric and Oceanic Sciences, Los Angeles, CA, US.

[9]Institute for the Study of Earth, Oceans and Space, University of New Hampshire, Durham, New Hampshire, US.

[10]Graduate School of Environmental Studies, Nagoya University, Nagoya, Japan.

Corresponding author: Becky Alexander (beckya@uw.edu)

Contents of this file

Text S1. Extended explanation on potential factors influencing bromine preservation in snowpack

If the photochemistry-dominated deep snow production is the major loss process of bromine from the snowpack, the extent of snow bromine preservation is at least partly determined by how quickly a snow layer is buried beneath the snow photic zone and isolated from solar radiation, similar to the photolysis-driven post-depositional loss of nitrate in snowpack (Röthlisberger et al., 20147; Winton et al., 2020; Akers et al., 2022). We assume that the depth of the snow photic zone is 30 cm, following Thomas et al. (2011) based on measurements for snowpack at Summit, Greenland (Galbavy et al., 2007). Table S3 summarizes the snowfall rate, the number of days needed to accumulate 10 cm of snow (assuming constant snowfall rate), and the duration of polar night at the six ice core locations.

AN has the highest snowfall rate and takes 28 days to accumulate 10 cm of snow. This means that about 44 cm snow is accumulated during the dark time of year (124 days), and at least 14 cm of this snow is buried underneath the snow photic zone (~3 times of e-folding depth, 30cm) at polar sunrise and this layer experiences minimal photochemical loss. In contrast, Greenland ice cores do not have snow layers that are completely isolated from the sunlight due to slower snow accumulation rate and lower latitude (fewer dark days).

To take seasonal variations in snowfall rate (Fig. S8) into consideration, Table S4 calculated the depth of snow accumulated during polar night period for each ice core, based on monthly mean snow accumulation rate from MERRA2 reanalysis in year 2007 and 2008. Only AN in 2008 has accumulated over 30 cm of snow during darkness, and Greenland ice cores accumulate a maximum of 16 cm (NEEM_2011_S1 in 2007) during darkness. Therefore, even if none of these ice core sites have snow layers completely isolated from the sunlight (e.g. year 2007), AN would still be the best preserved ice core among the six ice core sites.

A second factor that may regulate snowpack bromine release is the relative contribution of dry and wet deposition, which we hypothesize to have an effect on the location of impurities in snow grains. Snow impurities, including bromide, can reside in different locations based on snow formation and evolution processes. These locations include bulk and surface of ice crystals, grain boundaries, liquid brines, and in aerosol particles trapped in snow (Bartels-Rausch et al., 2014; Domine et al., 2013). How chemical reactivity of impurities differs with different locations in snow grains remain highly uncertain (Domine et al., 2013). Dry deposited bromine will at least initially be located at the snow grain surface and thus is more exposed for surface reactions. Wet deposited bromine, on the other hand, may be less reactive, as it may be trapped in the bulk ice crystals through rimming, in airborne particles as ice condensation nuclei, or from scavenging process during precipitation (Beine et al., 2011; Domine et al., 2004). The fact that ice core bromine concentrations in these Arctic cores never reach zero suggests that there is some fraction of snow bromine that is isolated from photochemical reactions and is thus preserved, although essentially all (below detection limits) bromine is lost at some very low snow accumulation ice core sites on the East Antarctic Plateau where dry deposition probably dominates (McConnell et al., 2017). If wet deposition contains a significant proportion of bromine that is not photochemically reactive, it may be isolated from photochemical loss and thus preserved. Under this assumption, more wet deposition implies higher bromine preservation. Fig.S9 shows that the model

predicts that AN and ACT_11d have the highest fraction of bromine that is wet deposited. This may also explain the apparent preservation of bromine trends from the mid-latitude ice core in French Alps, Col du Dome (Legrand et al., 2021), which has a high fraction of wet deposited bromine (80% based on our model simulations).

Lastly, recent studies (Burd et al., 2017; Jeong et al., 2022; Kim et al., 2018) have shown that surface melting can effectively shut down snowpack bromine reactions in summertime. In warm years like 2007, this shut down mechanism occurs for AN and ACT_11d in July, leading to better preservation at these two sites (Fig. 4 and Table 3). As the frequency and duration of surface melting increases in the Greenland ice sheet under a warming climate (Colosio et al., 2021; Parizek & Alley, 2004), it is likely that snowpack bromine emission will be shut down during most of the sunlit period in Greenland locations. However, it is uncertain how excessive melt of surface snow and possible thaw-refreezing cycles will impact ion re-distribution and snow morphology, and thus the chemical reactivity of snow impurities in the future.

Text S2. Extended explanation of change point analysis.

Figure S2 shows the Br_{enr} values from the six Arctic ice cores since the pre-industrial along with Bayesian Change Point model results. Only AN has a high probability for significant trends in Br_{enr}, increasing from 1930 to 1975 at a rate of 0.079 ± 0.009 per year, decreasing afterwards at a rate of −0.230 ± 0.101. NGT_B19 has some low-probability change points, with the largest one (around 1960) driven by an outlier value, and there is no significant difference in trends before and after the outlier. A rate of change of 0.004 ± 0.005 is found for NGT_B19 over the entire record, indicating there is no significant long-term trend either. For the other four Greenland ice cores, no change point is identified by any of the 500 sampled solutions during Bayesian Change Point analysis, and the rate of changes over the whole ice core time period are similar to variations, with the calculated trends over the entire record being 0.118 ± 0.103 for ACT_11d, 0.000 ± 0.010 for NEEM_2011_S1, −0.002 ± 0.004 for Tunu, and 0.003 ± 0.005 for Summit.

Figure S3 shows that the statistical analysis detects change points in both AN and Tunu with probabilities greater than 10%. AN Br_{exc} increased from 1930 to 1975, with a rate of change of 0.114±0.033 $ng \cdot g^{-1} \cdot yr^{-1}$, and decreased after 1975 with a rate of −0.156±0.033 $ng \cdot g^{-1} \cdot yr^{-1}$. Tunu Br_{exc} has a relatively stable trend before the change point at 1958, with a rate of change of −0.001±0.000 $ng \cdot g^{-1} \cdot yr^{-1}$ between 1750 and 1958. After 1958 Br_{exc} quickly increased until 1962 (0.062±0.031 $ng \cdot g^{-1} \cdot yr^{-1}$), then slightly decreased (−0.002±0.002 $ng \cdot g^{-1} \cdot yr^{-1}$) since then. Overall Br_{exc} at Tunu shows a rate of change of 0.000±0.000 $ng \cdot g^{-1} \cdot yr^{-1}$ throughout the entire record. No significant change points nor trends (0.000±0.000 $ng \cdot g^{-1} \cdot yr^{-1}$) over the entire record are detected for Br_{exc} at NGT_B19. Change points detected in NEEM_2011_S1 and ACT_11d are driven by outliers and Br_{exc} at these two sites show no long-term trends (0.001±0.000 $ng \cdot g^{-1} \cdot yr^{-1}$ for both sites). Summit sees a group of potential change points between 1855 and 1900, but none of them show a probability larger than 10%. There is a minor decreasing trend from 1750 to 1850 (−0.001±0.000 $ng \cdot g^{-1} \cdot yr^{-1}$), and a minor increasing trend from 1900 to the end of the core (0.001±0.000 $ng \cdot g^{-1} \cdot yr^{-1}$).

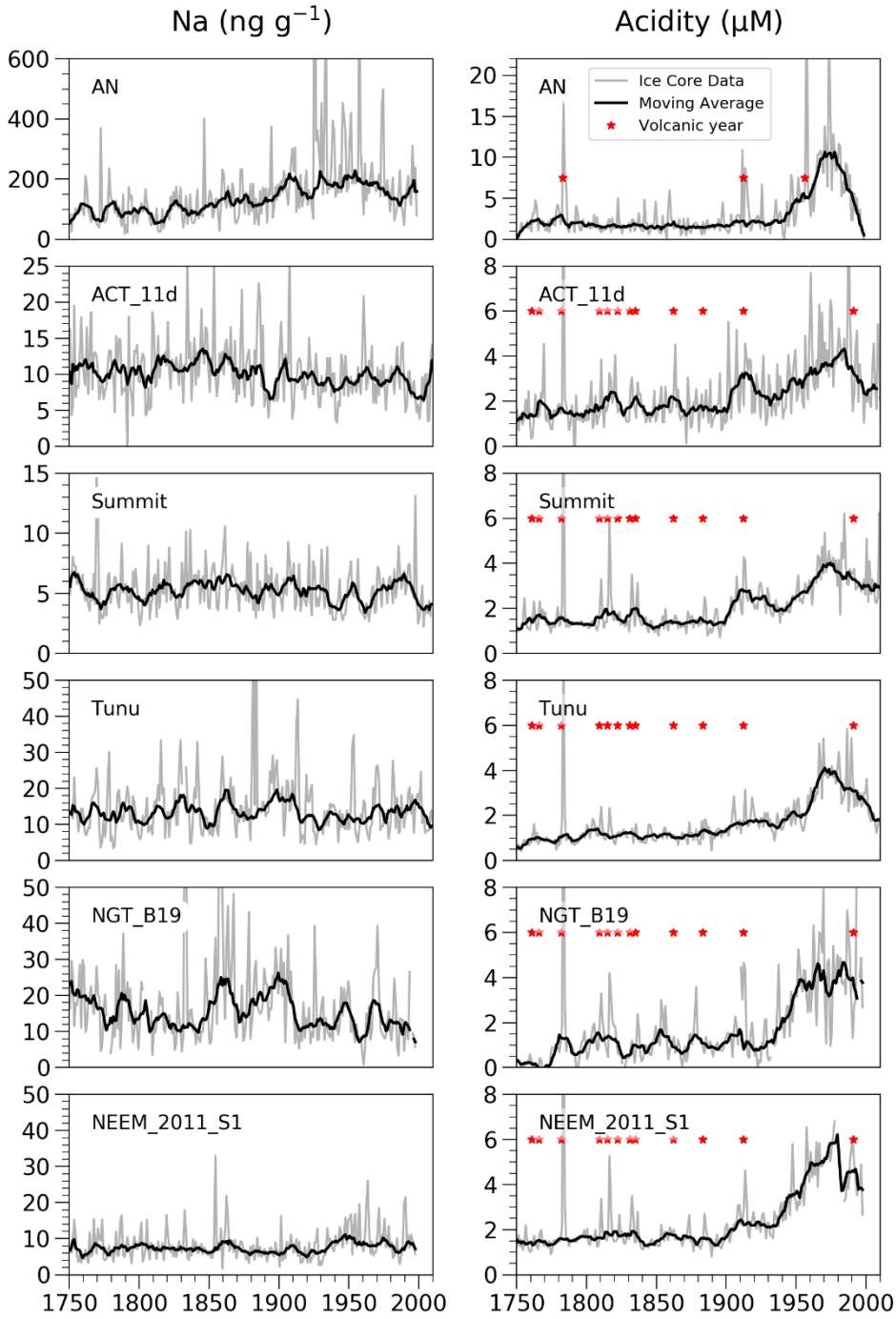

Figure S1 Ice core sodium (left) and acidity concentrations (right) in Akademii Nauk, ACT_11d, Summit, Tunu, NGT_B19, and NEEM_2011_S1 ice cores. Gray lines are the measured annual ice core concentrations, and black lines are the 9-year running average of the concentrations or calculations, with outliers outside of 1.5×IQR (interquartile range) removed. Red stars mark the large and moderate volcanic years identified in previous studies. Specifically, Opel et al. (2013) identified volcanic eruptions at Laki in 1783, Katmai in 1912, and Bezymianny in 1956 for AN, and those for

Greenland ice cores are based on Cole-Dai et al. (2013) and Sigl et al. (2013) as described in Zhai et al., 2021 Text S2.

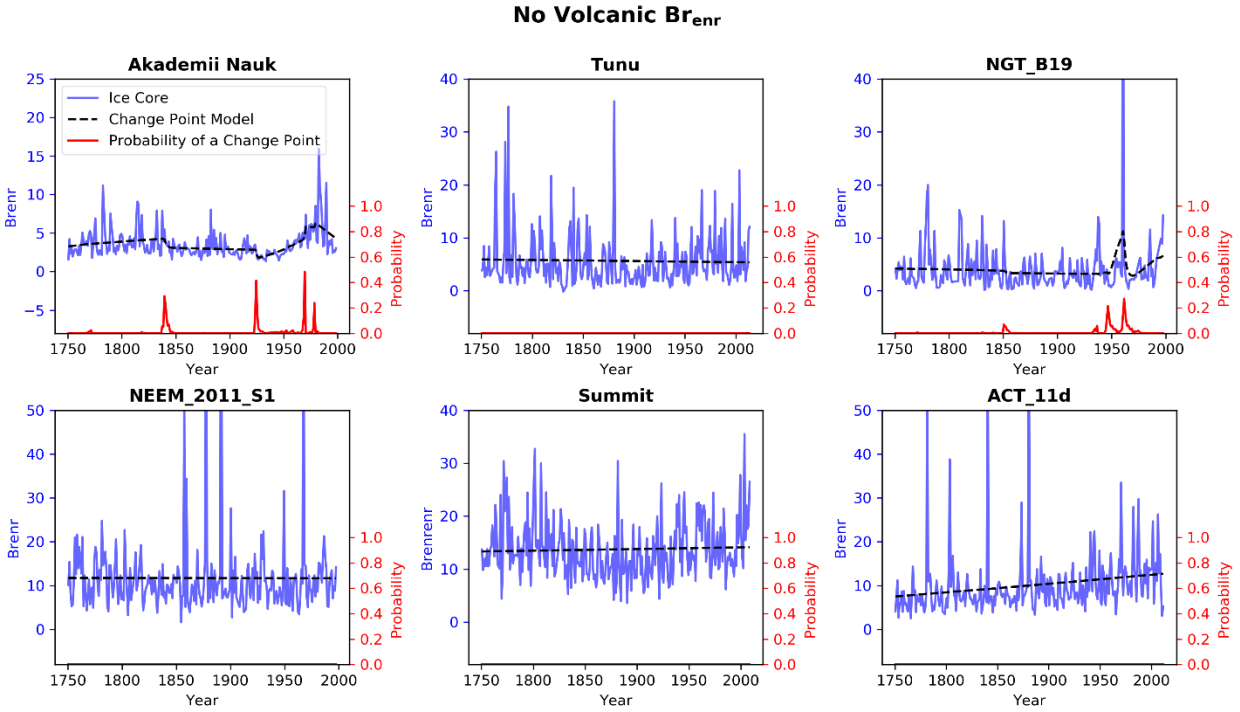

Figure S2. Br_{enr} records and trend analysis since year 1750 from six Arctic ice cores. Blue lines are ice core Br_{enr} values calculated based on ice core measurements of sea-salt sodium and bromine, with previously identified volcanic years removed (Opel et al., 2013; Cole-Dai et al., 2013; Sigl et al., 2013). Dashed black lines are the model predicted trends by the Bayesian Change Point algorithm. The heights of red spikes at the bottom of each panel indicate the probability of a potential change point. Tall, narrow spikes suggest relative certainty in the timing of a change point, where shorter and wider spikes suggest more uncertainty. No spikes are visible if no change points are identified by any of the 500 sampled solutions.

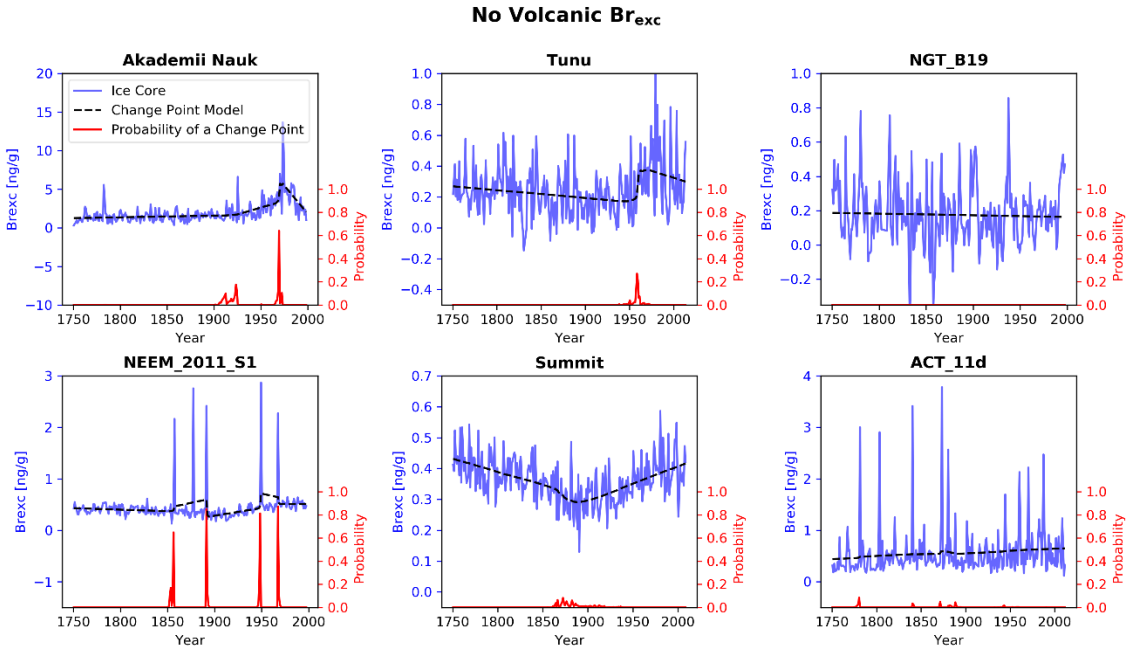

Figure S3. Similar to SI Figure S2 but for Br_{exc}.

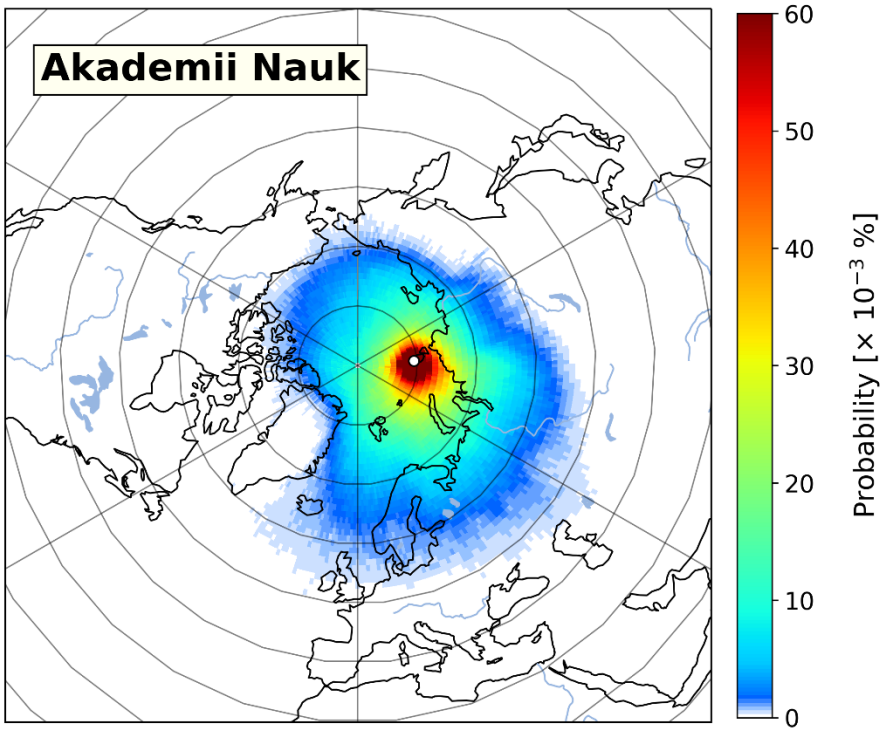

Figure S4 5-day back trajectory probability at Akademii Nauk calculated by the HYSPLIT model for the time period 1959-2010. The Akademii Nauk ice core site is marked as an open circle. Details of the HYSPLIT model parameters and settings are described in Zhai et al. (2021).

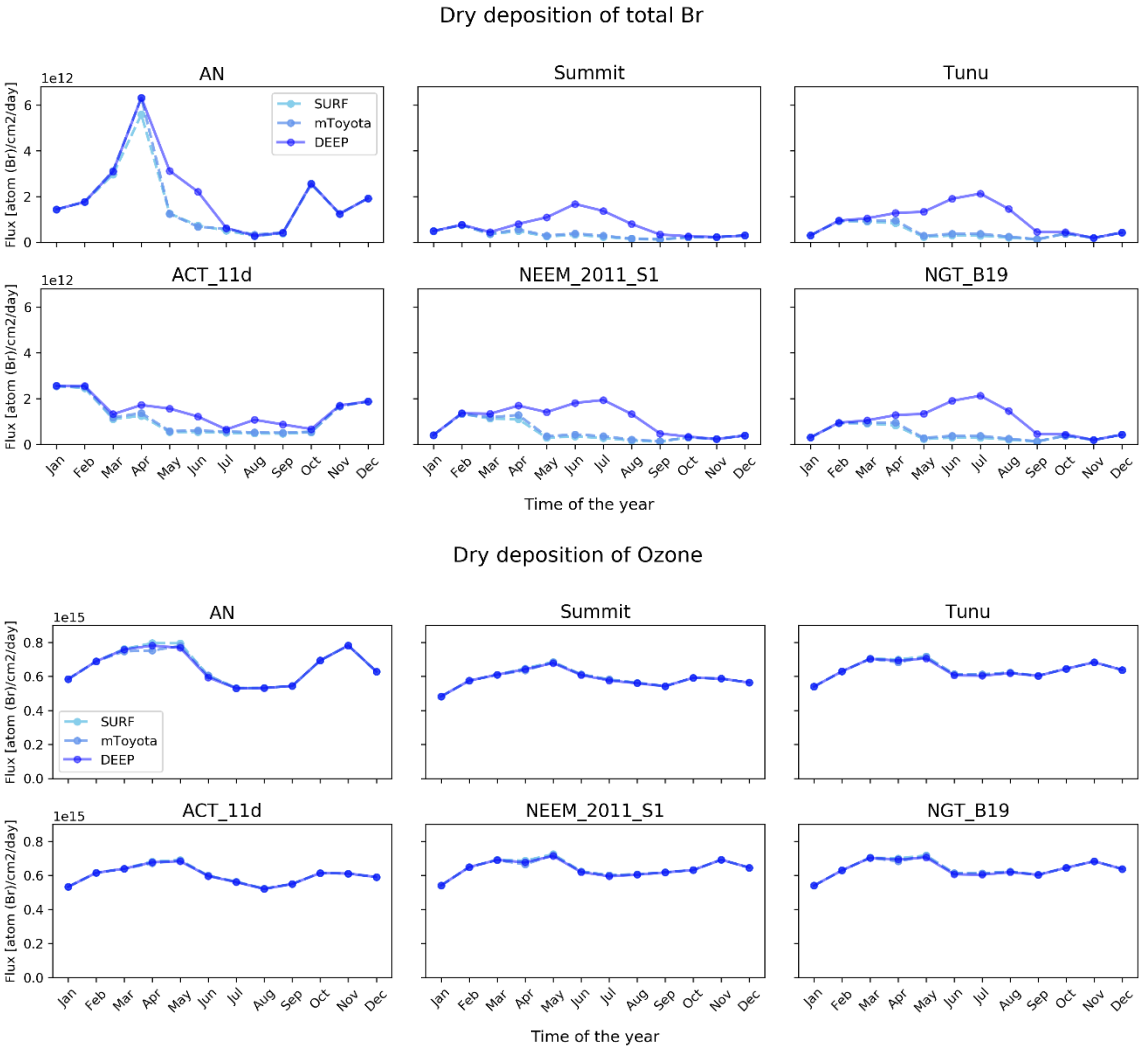

Figure S5. Modeled monthly mean dry deposition fluxes of total bromine (Br_y + sea salt Br^-) (top panels) and ozone (bottom panels) in the three simulations for the six ice core locations in year 2007.

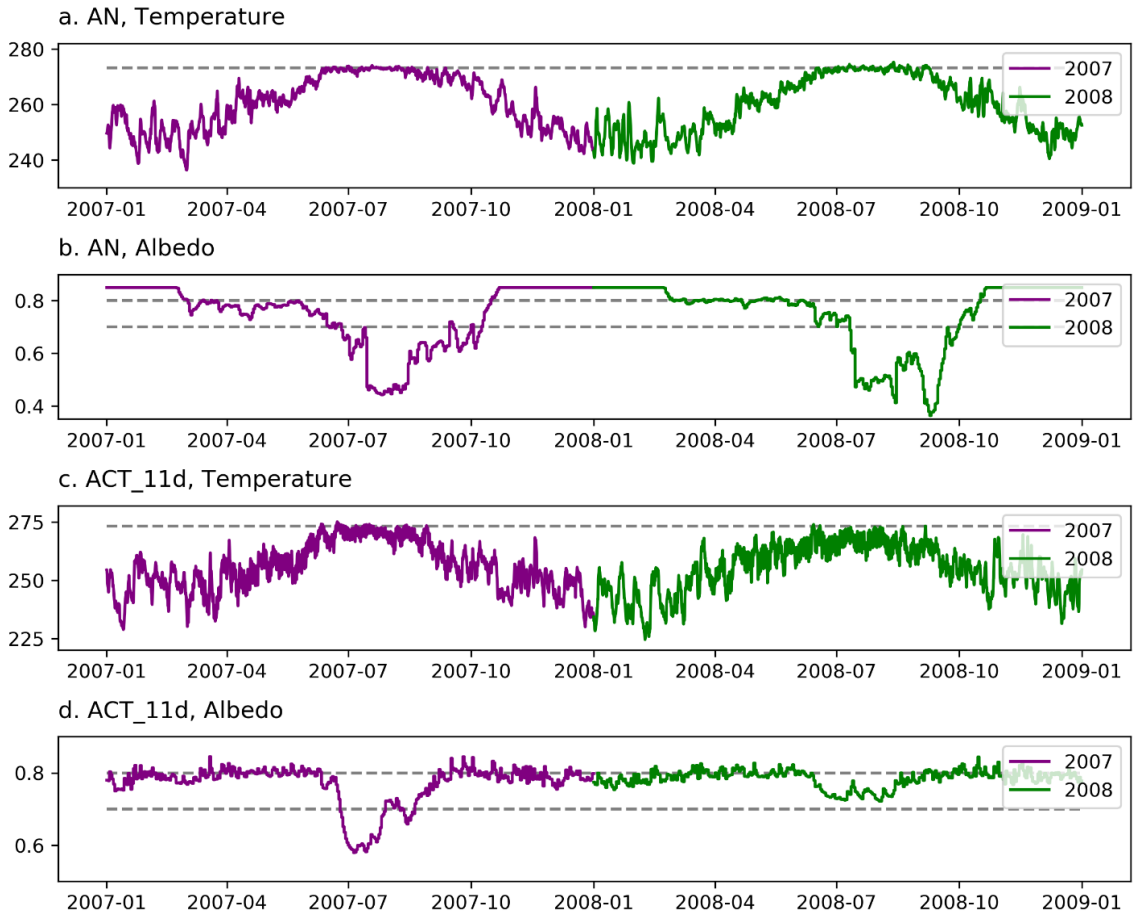

Figure S6. MERRA2 daily 2-meter air temperature (a, c) and surface albedo (b, d) at AN (a, b) and ACT_11d (c, d) for year 2007 and year 2008. Dashed gray lines mark either the temperature threshold of 273.15K, or the albedo values of 0.8 and 0.7. Snow bromine emission mechanisms are shut down when temperature goes above 273.15K or surface albedo is below 0.7 in this study.

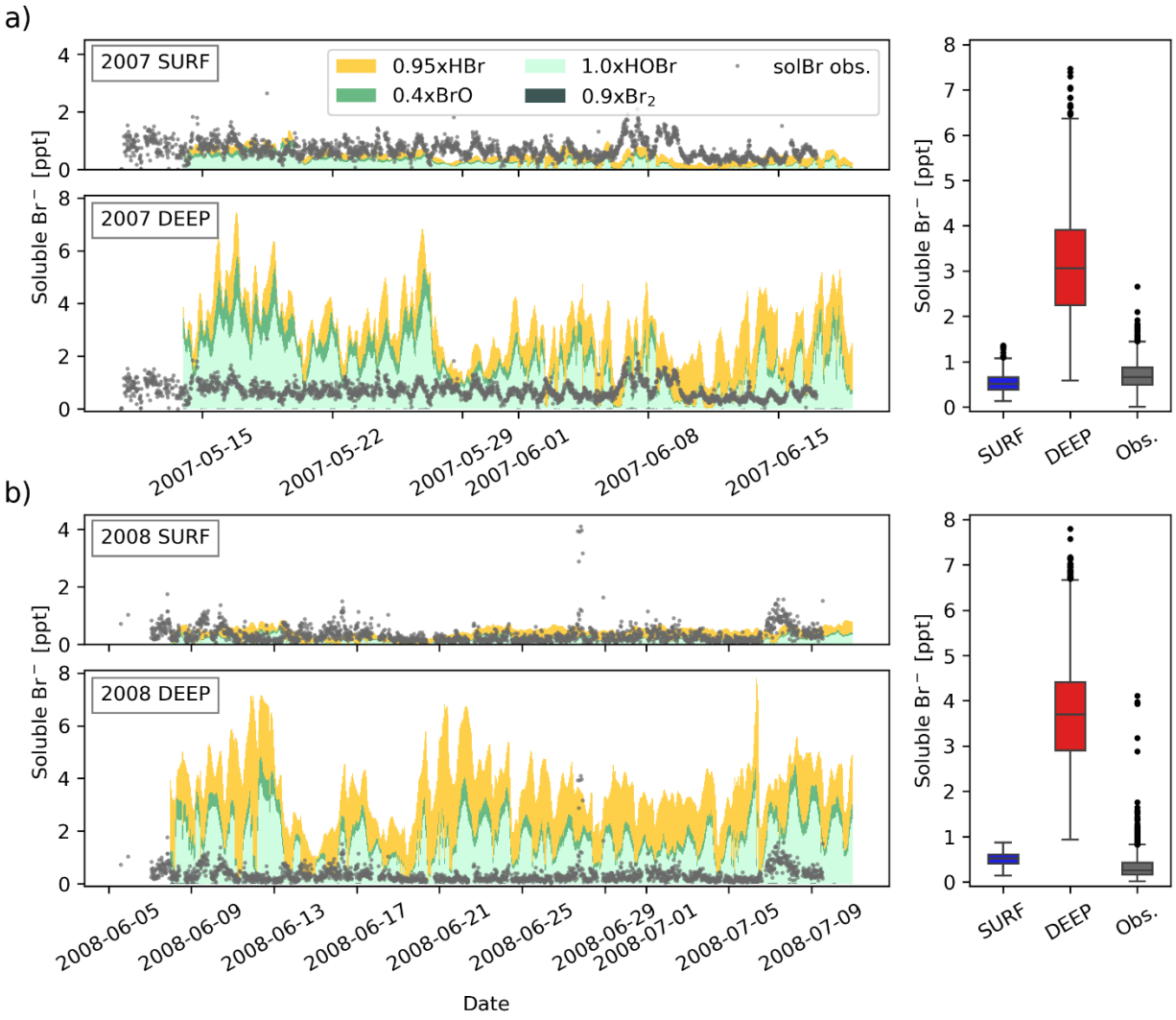

Figure S7 Comparison between the modeled hourly surface soluble bromide concentrations at Summit during a) May–June in 2007 and b) June–July in 2008 from SURF and DEEP simulations, and the Mist Chamber observed soluble bromide concentrations from Dibb et al. (2010). Soluble bromide is defined as in Liao et al. (2012), where $[Br^-] = 0.9[Br_2] + 1.0[HOBr] + 0.4[BrO] + 0.95[HBr]$. $0.9 \times Br_2$ is minimal compared to other constituents and is barely visible in the plot. SURF modeled mean soluble bromide is 0.5 ppt for both 2007 and 2008 seasons, similar to those reported in Dibb et al. (2010).

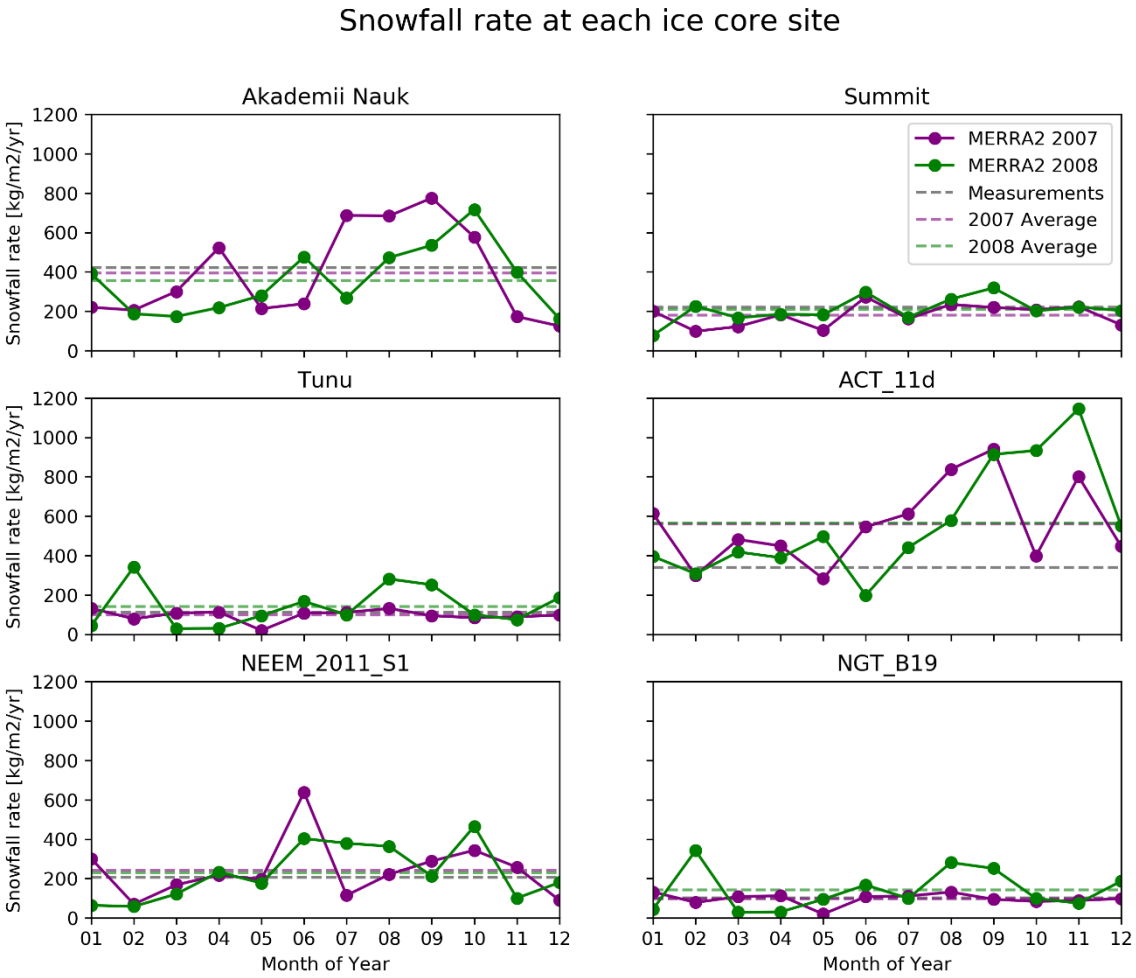

Figure S8. MERRA2 monthly snowfall rate at each ice core location for year 2007 (solid purple lines) and 2008 (solid green lines). Dashed gray lines mark the annual average snowfall rate calculated based on ice core records, and dashed purple and green lines are annual average snowfall rate from MERRA2 for year 2007 and 2008, respectively.

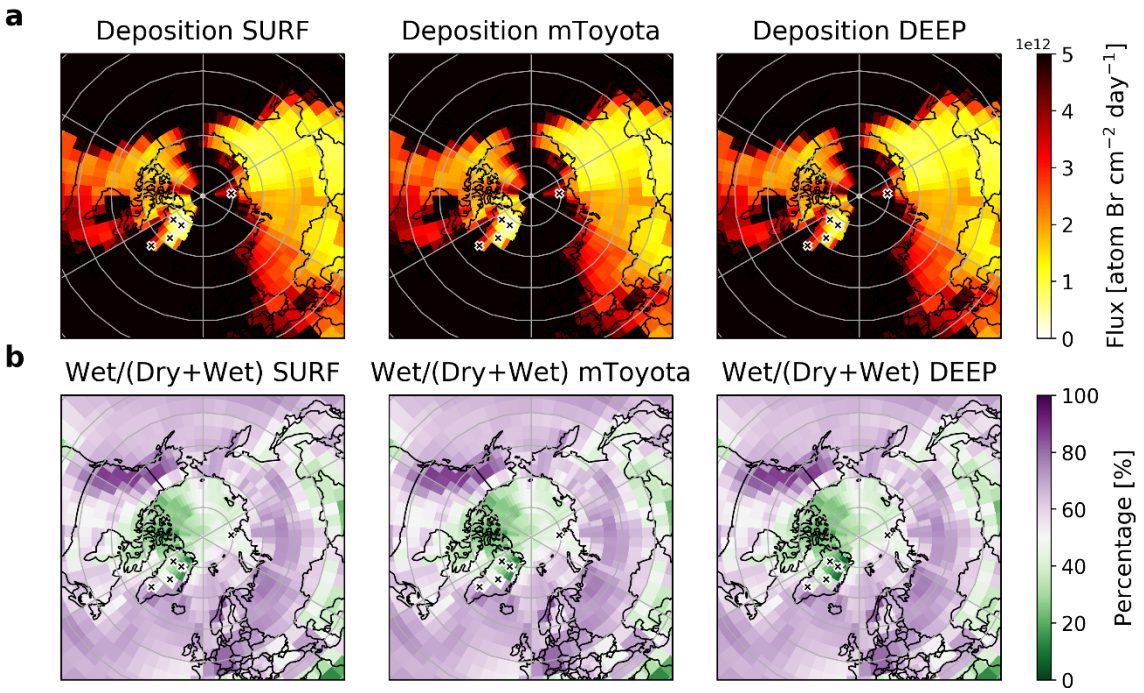

Figure S9. Simulated Arctic spatial distribution of annual mean a) total bromine deposition, and b) percentage of bromine wet deposition in total bromine deposition from the 3 simulations, SURF, mToyota, and DEEP. Red stars mark the ice core locations.

Table S1. Snowpack-air exchange fluxes of total bromine (total deposition, emission, net upward flux, and post-depositional loss) at the six ice core locations calculated from the mToyota simulation.

Ice core	Total deposition [atom Br cm^{-2} day^{-1}]	Emission (Br_2+BrCl) [atom Br cm^{-2} day^{-1}]	Net upward flux [atom Br cm^{-2} day^{-1}]	Post-depositional loss (Emission / Deposition)
AN	3.4×10^{12}	7.1×10^{11}	-2.7×10^{12}	21%
Summit	4.6×10^{11}	1.1×10^{11}	-3.4×10^{11}	25%
Tunu	5.1×10^{11}	1.2×10^{11}	-3.9×10^{11}	24%
ACT_11d	2.3×10^{12}	3.1×10^{11}	-2.0×10^{12}	13%
NEEM_2011_S1	7.7×10^{11}	1.4×10^{11}	-6.3×10^{11}	18%
NGT_B19	5.1×10^{11}	1.2×10^{11}	-3.9×10^{11}	24%

Table S2. Comparison of ice-core and SURF model-calculated annual mean concentrations of snow bromide

Ice core	Ice-core snow bromide (ng g^{-1})	Modeled snow bromide (ng g^{-1})
AN	2.7±1.3	4.04
Summit	0.4±0.1	1.16
Tunu	0.3±0.2	2.37
ACT_11d	0.6±0.5	1.93
NEEM	0.5±0.3	1.43
NGT_B19	0.3±0.2	2.37

Table S3. Comparison of the annual mean snowfall rate and duration of polar night at the six ice cores in this study. 30 cm is the snow photic zone depth.

	Akademii Nauk	Summit	Tunu	ACT_11d	NEEM_2011_S1	NGT_B19
Annual mean snowfall rate [kg m^{-2} yr^{-1}]	421	222	112	339	206	101
Time to accumulate 30cm snow [days]	84	159	312	105	171	348
Polar night	Oct.20 – Feb.21	Nov.15 – Jan.26	Oct.27 – Feb.14	≥2 hours daylight	Oct.29 – Feb.12	Oct.27 – Feb.14
Days in dark [#]	124	72	110	0	106	110

Table S4. Snow depth accumulated during polar night at the six ice cores in this study based on MERRA2 monthly averaged snowfall rate in 2007 and 2008.

		Akademii Nauk	Summit	Tunu	ACT_11d	NEEM_2011_S1	NGT_B19
Snow depth accumulated in dark days (cm)	2007	20	10	9	0	16	9
	2008	31	9	11		9	11